



ALMA MATER STUDIORUM
UNIVERSITÀ DI BOLOGNA

ARCHIVIO ISTITUZIONALE
DELLA RICERCA

Alma Mater Studiorum Università di Bologna Archivio istituzionale della ricerca

Δ 1 -Pyrroline-5-carboxylate synthetase (P5CS) deficiency: An emergent multifaceted urea cycle-related disorder

This is the final peer-reviewed author's accepted manuscript (postprint) of the following publication:

Published Version:

Marco-Marín, C., Escamilla-Honrubia, J.M., Llácer, J.L., Seri, M., Panza, E., Rubio, V. (2020). Δ 1 -Pyrroline-5-carboxylate synthetase (P5CS) deficiency: An emergent multifaceted urea cycle-related disorder. JOURNAL OF INHERITED METABOLIC DISEASE, 43(4), 657-670 [10.1002/jimd.12220].

Availability:

This version is available at: <https://hdl.handle.net/11585/725093> since: 2020-02-13

Published:

DOI: <http://doi.org/10.1002/jimd.12220>

Terms of use:

Some rights reserved. The terms and conditions for the reuse of this version of the manuscript are specified in the publishing policy. For all terms of use and more information see the publisher's website.

This item was downloaded from IRIS Università di Bologna (<https://cris.unibo.it/>).
When citing, please refer to the published version.

(Article begins on next page)

Δ^1 -Pyrroline-5-carboxylate synthetase (P5CS) deficiency: An emergent multifaceted urea cycle-related disorder.

Clara Marco-Marín,^{1,2,*} Juan M. Escamilla-Honrubia,^{1,2} José L. Llácer,^{1,2} Marco Seri,^{3,4}
Emanuele Panza,³ and Vicente Rubio^{1,2,*}

Affiliations: ¹Instituto de Biomedicina de Valencia of the CSIC, Valencia, Spain;

²Centro para Investigación Biomédica en Red sobre Enfermedades Raras CIBERER-

ISCIII, Valencia, Spain; ³Department of Medical and Surgical Sciences, University of

Bologna; ⁴Medical Genetics Unit, S. Orsola-Malpighi University Hospital, Bologna,

Italy

This review was invited as a part of the JIMD issue on Ureagenesis Defects: Novel Models and Treatment Options that was the outcome of a focused meeting on this topic held in Pontresina (Switzerland) 19-21 March 2018

***Send correspondence to:**

Clara Marco-Marín and to Vicente Rubio

Instituto de Biomedicina de Valencia (IBV-CSIC) and CIBERER

C/ Jaime Roig 11. Valencia-46010, Spain

cmarco@ibv.csic.es rubio@ibv.csic.es

Phone: +34 963391760 Telefax: +34 963690800

Word count. Summary: 250 words

Text: 3901 words

Number of Figures and Tables:

Main text: 4 figures

Supplementary Material: 1 figure and 1 table

Summary. The bifunctional homooligomeric enzyme Δ^1 -pyrroline-5-carboxylate synthetase (P5CS) and its encoding gene *ALDH18A1* were associated with disease in 1998. Two siblings who presented paradoxical hyperammonemia (alleviated by protein), mental disability, short stature, cataracts, cutis laxa and joint laxity, were found to carry biallelic *ALDH18A1* mutations. They showed biochemical indications of decreased ornithine/proline synthesis, agreeing with the role of P5CS in the biosynthesis of these amino acids. Of 32 patients reported with this neurocutaneous syndrome, 21 familial ones hosted homozygous or compound heterozygous *ALDH18A1* mutations, while 11 sporadic ones carried *de novo* heterozygous *ALDH18A1* mutations. In 2015-2016 an upper motor neuron syndrome (spastic paraparesis/paraplegia SPG9) complicated with some traits of the neurocutaneous syndrome, although without report of cutis laxa, joint laxity or herniae, was associated with monoallelic or biallelic *ALDH18A1* mutations with, respectively, dominant and recessive inheritance. Of fifty SPG9 patients reported, 14 and 36 (34/2 familial/sporadic) carried, respectively, biallelic and monoallelic mutations. Thus, two neurocutaneous syndromes (recessive and dominant cutis laxa 3, abbreviated ARCL3A and ADCL3, respectively) and two SPG9 syndromes (recessive SPG9B and dominant SPG9A) are caused by essentially different spectra of *ALDH18A1* mutations. On the bases of the clinical data (including our own prior patients' reports), the *ALDH18A1* mutations spectra, and our knowledge on the P5CS protein, we conclude that the four syndromes share the same pathogenic mechanisms based on decreased P5CS function. Thus, these syndromes represent a continuum of increasing severity (SPG9A<SPG9B<ADCL3≤ARCL3A) of the same disease, P5CS deficiency, in which the dominant mutations cause loss-of-function by dominant-negative mechanisms.

Take-home message. *ALDH18A1* gene mutations causing deficiency of the *ALDH18A1*-encoded bifunctional ornithine/proline biosynthesizing enzyme P5CS result in four syndromes that represent different degrees of severity of a single disease entity, P5CS deficiency, of which two syndromes result from dominant mutations that act by dominant negative mechanisms.

Contributions of individual authors

CM-M, JE-H, EP, MS and VR conceived the study, collected literature data on the patients' clinical descriptions, systematized, analyzed and interpreted these data. CM-M, JE-H and VR made inferences on the mechanisms of inheritance based on structural reasoning and on the pathogenic mechanism by loss-of function. CM-M, JLL and VR, analyzed the consequences of the mutations on the enzyme structure and function. VR and CM-M generated the figures and wrote the manuscript, and all the authors read it and made contributions to improve its writing.

Corresponding authors: Clara Marco-Marín and Vicente Rubio

Competing interests: Clara Marco-Marín, Juan M. Escamilla-Honrubia, José L. Llácer, Marco Seri, Emanuele Panza, and Vicente Rubio declare that they have no potential conflict of interest.

Funding:

Grant of the Spanish Government (MINECO BFU2017-84264-P): “Cerrando cuentas pendientes sobre biosíntesis de arginina/urea y sus errores congénitos, y sobre regulación de nitrógeno y sus implicaciones biomédicas” (Clara Marco-Marín and Vicente Rubio). Grant of the Fundación Inocente Inocente (Vicente Rubio).

Grant of American Spastic Paraplegia Foundation: ”Understanding Hereditary Spastic Paraplegia: in vivo models to identify pathogenetic mechanism and therapeutic targets for SPG9.” (Emanuele Panza)

The authors confirm independence from the sponsors; the content of the article has not been influenced by the sponsors.

Ethics approval. This work is a review and does not contain any human or animal studies performed by any of the authors. No ethical approval is needed.

Keywords. *ALDH18A1* gene-related disorders. Cutis laxa type III. Hereditary spastic paraplegia type 9. ARCL3A. ADCL3. SPG9A. SPG9B.

1. Introduction

The bifunctional enzyme Δ^1 -pyrroline 5-carboxylate synthetase (P5CS) (EC 1.2.1.41 & 2.7.2.11) and its encoding gene *ALDH18A1* (10q24.1) (Fig. 1A, B) were associated with disease in 1998¹, when homozygous *ALDH18A1* mutations were found in two siblings presenting paradoxical hyperammonemia (alleviated by protein intake), mental disability, short stature, cataracts, cutis laxa, joint laxity and biochemical indications of decreased ornithine and proline synthesis. Twenty one patients from 14 families have been reported¹⁻¹⁴ with biallelic *ALDH18A1* mutations associated to this neurocutaneous syndrome called autosomal recessive cutis laxa type IIIA (ARCL3A; MIM #219150) (Figs. 1C, top and 1D; Supplementary Table S1, rows in darker red hue). ARCL3A usually has early onset and can be very severe, presenting cutis laxa, mental disability, connective tissue weakness (joints hypermobility and dislocations, pes planum, inguinal herniae) and variable degrees of progeroid facies and of intrauterine and postnatal growth restriction leading to short stature. Cataracts and/or corneal clouding usually occur, while failure to thrive, gastroesophageal reflux with frequent vomiting, skeletal abnormalities and osteopenia are also observed (Fig. 1D). Plasma levels of one or several of the four amino acids proline, arginine, citrulline and ornithine can be low-normal or decreased.^{1,2-4,7,8,10}

In 2012 a sporadic neonatal patient was reported¹⁵ with a typical ARCL3A presentation except for his hosting of a *de novo* *ALDH18A1* missense mutation together with an inherited benign variant (Table S1, family 5), strongly suggesting a dominant nature of the *de novo* mutation. Ten additional sporadic patients have been reported¹⁶⁻¹⁸ with monoallelic dominant *ALDH18A1* pathogenetic variants and cutis laxa type III presentation (Fig. 1C, second panel from top, and Fig. 1D; and Table S1, rows in lighter red hue) leading to the definition of ADCL3 (MIM #616603).

Greater clinical complexity became patent in 2015-2016, when heterozygous *ALDH18A1* missense mutations were associated^{19,20} with complicated spastic paraplegia termed SPG9A (MIM #601162). Of 36 patients studied¹⁹⁻²² 34 familial cases ranged in five families, while two cases were sporadic (Figs. 1C, bottom panel and 1D; Table S1, light blue rows). A recessively inherited form of this motor presentation associated to biallelic *ALDH18A1* mutations, called SPG9B (MIM # 616586) has also been found in 14 studied patients from eight families^{19,23-27} (Figs. 1C third panel from top, and Fig. 1D; Table S1, rows in darker blue). SPG9A and SPG9B are characterized by an upper motor neuron syndrome generally of later onset, with variable degrees of weakness (sometimes mild enough in SPG9A to be manifested, in females, only during pregnancy, reverting afterwards²¹; pregnancy-associated initial manifestations without postpartum reversion has also been reported in SPG9A²²), progressive spastic limb paresis usually complicated (particularly in SPG9B²⁶) with learning disability, growth retardation, dysmorphic features, microcephaly and/or cyclic vomiting and bilateral cataracts, but without report of cutis laxa, joint hypermobility or herniae (Fig. 1D). Low-normal or decreased plasma urea cycle amino acids and/or proline have been reported in some patients^{19,20,23,24}.

The association with *ALDH18A1* mutations of two syndromes (neurocutaneous and motor) having each one of them either dominant or recessive inheritance, calls for clarification of the underlying mechanisms for this diversity. We provide here an evidence-based unifying view founded on the concept of a disease continuum of increasing severity in the order SPG9A<SPG9B<ADCL3≤ARCL3A corresponding to progressively increasing loss of P5CS function, in which the dominant forms result from loss of function due to dominant negative mechanisms.

2. P5CS: a crucial catalyst for *de novo* synthesis of ornithine and proline

Ornithine is crucial for ammonia detoxification by the urea cycle. Although not consumed in this cycle, it is scavenged mainly by oxidation of ornithine-derived glutamate, by conversion to putrescine or to proline, or by incorporation into body proteins mainly as arginine (but also as ornithine-derived proline, glutamate and glutamine) (Fig. 2A). Thus, it must be replenished by food intake (mainly as arginine) or by *de novo* synthesis (revised in²⁸; Fig. 2B). This synthesis occurs from glutamate, taking place in the mucosal cells of the small intestine, with subsequent conversion of *de novo* made ornithine to either arginine (children of <5 years)²⁹ or citrulline (beyond 5 years).^{28,30} These amino acids are exported to blood, with conversion of the citrulline to arginine by the kidney, which releases arginine to the circulation. Circulating arginine can enter the liver and replenish decaying ornithine levels.³⁰

The coexistence in enterocytes' mitochondria of^{28,29,31-33} P5CS, ornithine aminotransferase (OAT), ornithine transcarbamylase (OTC), carbamoyl phosphate synthetase (CPS1) and the CPS1 activating enzyme N-acetyl-L-glutamate synthase (NAGS) (Fig. 2B) strongly favors *de novo* synthesis of citrulline. Glutamate is abundant in enterocytes and promotes ornithine synthesis by the concerted action of P5CS and OAT, two enzymes for which glutamate is a substrate. OTC, by trapping ornithine as citrulline using CPS1-made carbamoyl phosphate from the abundant intestinal cell ammonia, pulls further the OAT reaction in the direction of ornithine synthesis.

Many other cell types host in their mitochondria P5CS and OAT^{28,31} (Fig. 2C). However, unlike enterocytes, they lack NAGS, CPS1 and OTC. While in these cells OAT is used to catabolize ornithine (as proven in OAT deficiency, which gives very high ornithine levels²⁸), the P5CS is used to make proline *de novo* (Fig. 2C).^{2,28,31} The P5CS polypeptide is composed of N-terminal glutamate 5-kinase (G5K) and C-terminal

glutamyl-5-phosphate reductase (G5PR) moieties (Fig. 1B).³¹ The P5CS oligomer (believed to be a tetramer¹⁶ or hexamer²⁰) makes glutamate-5-semialdehyde (G5S) from glutamate in two sequential steps (Fig. 2D). Glutamate is first phosphorylated by the G5K component, using ATP. The resulting unstable³⁴ glutamyl-5-phosphate (G5P) is reductively dephosphorylated to G5S in an NADPH-requiring reaction catalyzed by the G5PR component (possibly of another subunit, see below). In non-intestinal cells lacking OTC the unfavorable equilibrium of the OAT reaction leads to the lingering of the G5S made by P5CS and to its spontaneous cyclization to Δ^1 -pyrroline-5-carboxylate (P5C) (Fig. 2D).^{28,35} This last compound is reduced to proline in an NADPH-dependent reaction (Fig. 2C) catalyzed by the mitochondrial Δ^1 -pyrroline-5-carboxylate reductases PYCR1 and PYCR2³⁵⁻³⁷ (the letters composing the PYCR abbreviation are underlined). The role of PYCR1 in proline biosynthesis is well documented,³⁶ while PYCR2³⁷ may predominate functionally in the nervous system.

The key involvement of P5CS in the routes of *de novo* synthesis of both ornithine and proline (Fig. 2B,C) is reflected in the existence of two molecular forms of the P5CS polypeptide of 793 or 795 amino acids. The shorter form, resulting from the skipping of codons 238 and 239 by alternative splicing³¹ (Fig. 1B), is predominantly expressed in enterocytes, where it is committed to make ornithine (Fig. 2B), being controlled by feed-back inhibition by ornithine.³¹ The 2-residue longer form of P5CS is insensitive to ornithine and is prevalent in non-enteric cell types,^{2,31} where it is involved in proline synthesis (Fig. 2C).

3. *ALDH18A1*-related disorders can be manifestations of deficient production of ornithine and proline

Loss-of-function P5CS mutations should reduce or abolish *de novo* production of ornithine, citrulline, arginine and proline, explaining the decreased (although

inconstantly, possibly due to blurring by food intake and tissue catabolism) plasma levels of these amino acids in *ALDH18A1*-related syndromes^{1-4,7,8,10,13,15-17,19,20,23,24} (Fig. 3A). The ornithine needed for making urea can be limited in interprandial periods, explaining the paradoxical hyperammonemia observed in the first two reported ARCL3A patients.¹⁻³

Low proline synthesis might hamper production of the very abundant (~35% of the body protein mass) connective tissue proteins collagen and elastin, which are proline-rich (proline+hydroxyproline represent 25% and 14% of the mass of each of these proteins, respectively). This likely explains (Fig. 1D) the cutis laxa and connective tissue weakness and possibly also the bony alterations (dysmorphic features, osteopenia,^{3,6,11,15-17} etc), the vascular tortuosity^{5,15-18}, cyclic vomiting and even cardiac defects^{5,10,12,22} and mitral valve leaks^{19,26} observed in some of these patients. Indeed, elastic fiber alterations have been noted in skin biopsies of patients of *ALDH18A1*-associated syndromes.^{5-7,15} Alterations in collagen fiber bundle architecture have also been reported.^{5,15} The corneal clouding seen in the most severe ARCL3A cases^{5,10} has been linked to microanatomical corneal alterations affecting the extracellular matrix, which is largely collagenous in the cornea⁵. The cataracts have been attributed² to proline deficiency. This deficiency could restrict both protein synthesis and/or a proline-mediated redox cycle in which P5C, which is present in the lens, is a crucial component.²

Proline and hydroxyproline together represent about 12% of the whole body protein mass.³⁸ Therefore, poor *de novo* synthesis of proline may be detrimental for rapid growth in the final stages of fetal development and the first years of postnatal life and may contribute importantly to the intrauterine and postnatal growth restriction resulting in short stature in *ALDH18A1*-associated syndromes (Fig. 1D). The role of

proline is supported by the intrauterine growth restriction that is also observed in PYCR1 deficiency,^{6,7,36,39} a proline biosynthesis disorder which does not primarily affect ornithine synthesis. Interestingly, studies in cultured melanoma cells⁴⁰ showed that siRNA knockdown of P5CS dramatically increased cell doubling time, apparently because of general metabolic slowdown and inhibition of protein synthesis linked to activation of the general control nonderepressible 2 (GCN2) protein kinase. These effects were reversed by proline addition.

A negative impact on the mental status of subclinical chronic mild hyperammonemia cannot be excluded in *ALDH18A1*-related disorders. However, impaired local proline production in the nervous system may have a predominant role in the neurocognitive alterations, since PYCR1 and PYCR2 deficiencies^{6,7,36,37,39} (two pure disorders of proline synthesis) usually cause mental disability and even neuroanatomic alterations (e.g. corpus callosum thinning/atrophy^{36,37,41}) found in *ALDH18A1*-related syndromes. The mechanisms of these alterations remain to be ascertained, although restricted protein synthesis and reduced antioxidant protection in the central nervous system, both due to limited proline availability, might be important determinants.

Similarly, the pathophysiology of the upper motor neuron syndrome is uncertain. It was proposed to be linked to ornithine¹⁹ since it was not described in PYCR1 deficiency^{6,7,36}. Furthermore, spastic paraplegia also develops in patients of argininemia and of hyperornithinemia-hyperammonemia-homocitrullinuria (HHH),^{19,42,43} two syndromes in which, as in P5CS deficiency, there is mitochondrial ornithine deficiency. It has been speculated^{42,43} that autophagy and arginine/ornithine imbalance could be involved in causing the paraplegia manifestations. More studies are needed to substantiate these proposals and, particularly, to link mechanistically mitochondrial ornithine insufficiency and upper motor neurone syndrome.

Other pathogenic possibilities remain to be explored in these syndromes, such as the potential role of polyamines (of which ornithine is a key precursor, Fig. 2A), given the crucial role of polyamines for development⁴⁴. The close metabolic relations of proline, ornithine, glutamate and glutamine (Fig. 2A,C) should also be taken into account, particularly since seizures are frequent among these patients,^{3-5,7,8,10-13,15,19,23,24,26} and given the facts that glutamate is an excitatory and potentially neurotoxic neurotransmitter while γ -aminobutyric acid (GABA) derives from glutamate and is an inhibitory neurotransmitter. A new dimension to be explored was recently open when an important signalling role of proline and its metabolism that could affect even autophagy was reported.⁴⁵

4. Two syndromes reflecting different severities of the same disease process?

We propose here that the neurocutaneous and the spastic paraplegia syndromes represent, respectively, higher and lower degrees of severity of the same disorder corresponding to higher and lower degrees of loss of P5CS function. This functional loss is reflected in the parameters listed in Fig. 3A (some of them directly reflecting P5CS activity: rows 2, 4 and 5 of this figure), of which at least some have been reported for all four syndromes. A number of observations support a greater loss of P5CS function and higher severity of the presentation in ARCL3A and ADCL3 than in SPG9 presentations: 1) null *ALDH18A1* mutations were observed more frequently in ARCL3A than in SPG9B (respectively, null/missense mutation ratios, ~1:2 and ~1:5; Figs. 1C, 3B and Table S1); 2) three patients reported with biallelic obligatory null *ALDH18A1* mutations^{5,10} presented extremely severe ARCL3A, with two dying at ≤ 6 months of age (Table S1, families 29, 31 and 35; filled red dots in the left and central panels of Fig. 3 C); 3) all ADCL3 patients were sporadic cases¹⁶⁻¹⁸ while 34 of the 36 studied SPG9A patients were familial cases¹⁹⁻²³ (Fig. 1D; Table S1, light red and light

blue rows), indicating that the monoallelic mutations in ADCL3 but not in SPG9A caused too much disability to allow reproduction; 4) the age of disease onset was earlier, survival time was higher and disease duration was longer for pooled ARCL3A and ADCL3 patients than for pooled SPG9B and SPG9A patients (Fig. 3C); 5) the combined scores yielded by the Polyphen2 (<http://genetics.bwh.harvard.edu/pph2>) and MutPred2 (<http://mutpred.mutdb.org>) disease-causation prediction servers tended to be higher for single amino acid variants found in ARCL3A and ADCL3 than for variants found in SPG9 syndromes (Fig. 3D, left panel); and the scores for amino acid conservation for the residues replaced in ARCL3A and ADCL3 tended to be higher than for those replaced in SPG9B and SPG9A (Fig. 3D, right panel and Supplementary Fig. S1) in line with the fact that higher conservation is characteristic for more important residues for protein function or stability.

Fig. 1D illustrates in heat-plot style the existence of a true disease continuum for the four syndromes, which share most disease traits although with different observed frequencies depending on the syndrome. The most severe end of this continuum is represented by the cutis laxa syndromes, and, in particular, by the three patients that hosted biallelic obligatory null *ALDH18A1* mutations (Table S1, families 29, 31 and 35). These ARCL3A patients prove that lack of P5CS is not lethal in utero but that it consistently causes very important intrauterine growth restriction leading to very low birth weight (1.5, 1.8 and 1.4 kg in these three patients)^{5,10}, decreased body length and head circumference.^{5,10} Other characteristic features of these three patients were postnatal failure to thrive, bilateral corneal clouding (2 of the three cases^{5,10}) or very early cataract (the other case¹⁰), and the occurrence of thin, wrinkled, loose and semi-transparent skin with visible dermal vessels, very marked progeroid facial features, joint contractures and, later on, joint luxations and/or herniae. Skin ultrastructure, studied in

one of these patients, revealed abnormal elastic fibers.¹⁰ Clearly, these three patients represent the more florid and severe end of the disease continuum. At the lower severity end for most manifestations are the dominant forms of SPG9, which for the traits shared with the cutis laxa forms, exhibit lower frequencies of occurrence (among patients, families and genotypes, Fig. 1D). A patient-by-patient exemplification of the disease continuum is illustrated in Fig. 3E for global developmental delay/intellectual disability, essentially constant among the ARCL3A and ADCL3 patients, also observed in all but one SPG9B patient, but absent from all but one SPG9A patient.¹⁹⁻²² An exception to this continuum is the lack of report of cutis laxa and of most manifestations of connective tissue weakness (joint laxity/inguinal hernia; not shown separately) in SPG9A patients, strongly suggesting that above a certain P5CS activity level the connective tissue manifestations are either absent or are not prominent enough to be easily remarked. This may be particularly so for cutis laxa, which even in the florid cases tends to ameliorate with age.⁴

Concerning the upper motor neuron syndrome, it appears to be a nearly constant element of all *ALDH18A1*-related syndromes, given the finding of pyramidal signs and of tonus disturbance (hypotonia) in many patients with the cutis laxa syndromes. Given the low age of most of these cutis laxa patients and the severity of their manifestations, and since the motor syndrome appears to take time to develop, as noted for the SPG9 syndromes, the motor manifestations are not fully observed in most cutis laxa patients or are overshadowed by the early and more severe neurocutaneous presentations observed in the ARCL3A and ADCL3 syndromes. This delayed appearance of the complete motor syndrome is clearly illustrated in the first two patients (brother and sister) reported with ARCL3A. These patients have been followed for >10 years, showing progressively more prominent motor manifestations with time despite the fact

that the initial manifestations were those of the neurocutaneous syndrome.¹⁻³ Thus, while both patients could walk at 4 years of age, they lost the ability to walk when 12-15 years-old as a consequence of the motor syndrome with manifestation of severe pyramidal syndrome.³ In another ARCL3A family with four siblings of 21 to 4 years of age,⁴ the patients, although reported in less detail, also appear to manifest the motor syndrome after an initial cutis laxa presentation, leading to loss of ability to walk. In fact, motor disability occurred sooner in these six ARCL3A patients^{3,4} than in most SPG9B patients, and appeared more severe than in most SPG9A patients.

On the occasion of our reporting of two novel SPG9B patients, we recently showed that SPG9B is more severe than SPG9A.²⁶ In the case of ARCL3A and ADCL3, the patients' data suggests similar degrees of severity for these two syndromes, as exemplified with the severe presentations observed for some ADCL3 patients reported in detail,^{15,46} particularly a patient⁴⁶ presenting a florid clinical picture associated with total motor disability, who died at about 3 years of age (blue circle in Fig. 3C, middle panel). Motor disturbance was also reported for an ADCL3A patient¹⁸ who at 8 years of age was only able to walk with support. In any case, more ADCL3 patients must be identified before a sounder conclusion on differences in severity with ARCL3A can be attained. What appears clear is that the dominant cutis laxa presentations are more severe than SPG9 presentations and certainly much more severe than the SPG9A presentations (Fig. 1D).

5. Why dominant and recessive modes of inheritance?

The clinical similarities of ARCL3A and ADCL3 agree with the operation of the same disease mechanism for these two syndromes (different degrees of decrease in P5CS function) irrespective of the recessive or dominant inheritance. The same can be said for SPG9A and SPG9B. As already noted,¹⁹ the dominance cannot be attributed to

haploinsufficiency, since patients' parents carrying a null allele together with a wild type allele are healthy (e.g.^{5,10}). A dominant negative effect appears the most plausible mechanism for the dominance in ADCL3 and SPG9A^{15,16,19,20} (Fig. 4A). If P5CS is functional only when in oligomeric form,^{15,16,20} the incorporation of a subunit with a mutation could have a dominant negative effect if it disturbs the architecture of the hybrid oligomer composed of wild-type and mutant subunits, inactivating or decreasing the activity of the entire oligomer^{15,20}. This is best explained if in the normal P5CS oligomer the unstable³⁴ G5P intermediate must be channelled between the G5K and G5PR active centers of different subunits (Fig. 2D). The architectural defect caused by the incorporation of a subunit with a dominant mutation could either prevent the channelling or decrease its efficiency by altering the relations between G5K and G5PR active centers of different subunits (Fig. 4A). Detailed knowledge of the P5CS architecture and not only of the structures of the isolated G5K and G5PR components^{15,20} (Fig. 4B,C) is needed to explain in physical terms how this channelling occurs and how it can be hampered by certain mutations.

Only pathogenetic variants in which the mutant polypeptide is produced and is soluble and integrable into the oligomer can have dominant-negative effects (Fig. 4A). The formation of such hybrid mutant/wild-type oligomers was proven for dominant forms found in ADCL3,¹⁶ whereas evidence for architecturally disturbed oligomers was obtained for two dominant mutations found in SPG9A families.²⁰ In agreement with this pathogenetic mechanism, no mutations that abolish the production of the mutant protein (for example, truncating mutations) have been found in patients with the dominant presentations ADCL3 or SPG9A, while these mutations have been observed in patients having the recessive syndromes ARCL3A^{5,10,11,13,14} and SPG9B^{23,25} (Fig. 1C, 2B and Table S1).

There should be complete specificity on whether a missense mutations has a recessive or a dominant negative effect. Sequence variants that cause gross misfolding, with loss of the mutant subunit, or that inactivate active centers without disturbance of intersubunit interactions should be recessive (Fig. 4A and D), whereas dominant mutations should allow integration of the mutant subunit into the oligomer, altering the architecture of the P5CS oligomer (Fig. 4A). Indeed, among the 29 missense mutations found thus far in patients with *ALDH18A1*-associated syndromes, none occurred in both a recessive syndrome and a dominant one. Only one amino acid, Arg665, was substituted in recessive and dominant SPG9, to Gln in the first case and to Leu in the second. Furthermore, mutations recurring in unrelated individuals or families always were associated with the same type of inheritance, as best exemplified for the dominant mutations affecting codon 138 in *ADCL3*.^{16,17}

Dominant missense mutations might also be less numerous than those causing recessive inheritance, as they can only have a dominant effect if they do not cause gross misfolding and if they affect strategic points in the protein that are involved in intersubunit interactions. Indeed, among the 29 missense mutations identified in *ALDH18A1*-associated disorders the number of recessive ones (19) nearly doubles that of dominant ones (10) (Fig. 1C and Table S1). The distribution of the mutations is also very different for recessive and dominant mutations: six of the residues affected by dominant mutations map in the G5K component of the P5CS polypeptide and only two map in the G5PR component, possibly reflecting a predominant involvement of the G5K component in intersubunit interactions in the P5CS oligomer (Fig. 1D). Interestingly, in the inferred (from bacterial G5K⁴⁷) and experimental (see²⁶) respective structural models for the G5K and G5PR components of human P5CS, the residues

involved in dominant mutations are in the surface or close to it in superficial structural elements.²⁰

The distribution of the recessive missense mutations is also different for the neurocutaneous syndrome and for the motor syndrome, as might be expected for mutations causing, correspondingly, more and less loss of P5CS function. Particularly remarkable is the clustering of missense mutations towards the C-terminus of the G5PR component in the ARCL3A syndrome. The crystal structure of the dimer of this component (Fig. 4C,D) shows that these mutations map together towards the same zone of the protein, where the interaction domain of one subunit sits between the other two domains of the G5PR component of the other subunit, at the junction of these domains, conforming the active center of the G5PR component. Although the effects of these mutations have not been determined, it is tempting to propose that all them have as their major effect the inactivation of the G5PR component. However, misfolding effects cannot be excluded, particularly for Arg765, a residue likely helping stabilize the hybrid β -sheet formed between the oligomerization domain of a subunit and the catalytic domain of the other subunit.

6. Closing remarks.

We propose here a unifying view for *ALDH18A1*-associated disorders in which 1) the clinical manifestations are due to loss of P5CS function (P5CS deficiency); 2) the different presentations conform a disease continuum of decreasing severity from the cutis laxa forms ARCL3A and ADCL3 to the motor syndromes SPG9B and SPG9A; 3) specific mutations associate with a specific syndrome because they cause different degrees of enzyme deficiency depending on the mutation; and 4) the specific recessive or dominant character of each individual mutation reflects the respective lack or

existence of negative effects of the mutation on the architecture of the whole enzyme oligomer.

Further evidences for this unifying view could be obtained by developing genetically modified animal models (preferably mammalian models) for each one of the four human P5CS syndromes. In turn, the determination of the structure of human P5CS could provide insight into the specific mechanisms of intramolecular channelling of the G5P intermediate that is likely to be hampered by the dominant mutations, helping predict what mutations could have a dominant-negative effect and the intensity of such effect.

ACKNOWLEDGMENTS

We thank the American Spastic Paraplegia Foundation for the EP grant "Understanding Hereditary Spastic Paraplegia: in vivo models to identify pathogenetic mechanism and therapeutic targets for SPG9". VR and CM-M were supported by grants of the Fundación Inocente Inocente and of the Spanish Government (MINECO BFU2017-84264-P).

REFERENCES

1. Kamoun P, Aral B, Saudubray JM. A new inherited metabolic disease: Δ^1 -pyrroline 5-carboxylate synthetase deficiency. *Bull Acad Natle Med.* 1998;182:131-139.
2. Baumgartner MR, Hu CA, Almashanu S, et al. Hyperammonemia with reduced ornithine, citrulline, arginine and proline: a new inborn error caused by a mutation in the gene encoding Δ^1 -pyrroline-5-carboxylate synthase. *Hum Mol Genet.* 2000;9:2853-2858.

3. Baumgartner MR, Rabier D, Nassogne MC, et al. Δ^1 -pyrroline-5-carboxylate synthase deficiency: neurodegeneration, cataracts and connective tissue manifestations combined with hyperammonaemia and reduced ornithine, citrulline, arginine and proline. *Eur J Pediatr.* 2005;164:31-36.
4. Bicknell LS, Pitt J, Aftimos S et al. A missense mutation in *ALDH18A1*, encoding Δ^1 -pyrroline-5-carboxylate synthase (P5CS), causes an autosomal recessive neurocutaneous syndrome. *Eur J Hum Genet.* 2008;16:1176-1186.
5. Skidmore DL, Chitayat D, Morgan T, et al. Further expansion of the phenotypic spectrum associated with mutations in *ALDH18A1*, encoding Δ^1 -pyrroline-5-carboxylate synthase (P5CS). *Am J Med Genet A.* 2011;155A:1848-1856.
6. Zampatti S, Castori M, Fischer B, et al. De Barsy syndrome: a genetically heterogeneous autosomal recessive cutis laxa syndrome related to P5CS and PYCR1 dysfunction. *Am J Med Genet A.* 2012;158A:927-931.
7. Gardeitchik T, Mohamed M, Fischer B, et al. Clinical and biochemical features guiding the diagnostics in neurometabolic cutis laxa. *Eur J Hum Genet.* 2014;22:888-895.
8. Wolthuis DF, van Asbeck E, Mohamed M, et al. Cutis laxa, fat pads and retinopathy due to *ALDH18A1* mutation and review of the literature. *Eur J Paediatr Neurol.* 2014;18:511-515.
9. Handley MT, M egarban e A, Meynert AM, et al. Loss of *ALDH18A1* function is associated with a cellular lipid droplet phenotype suggesting a link between autosomal recessive cutis laxa type 3A and Warburg Micro syndrome. *Mol Genet Genomic Med.* 2014;2:319-325.

10. Fischer B, Callewaert B, Schröter P, et al. Severe congenital cutis laxa with cardiovascular manifestations due to homozygous deletions in *ALDH18A1*. *Mol Genet Metab.* 2014;112:310-316.
11. Stavropoulos DJ, Merico D, Jobling R, et al. Whole genome sequencing expands diagnostic utility and improves clinical management in pediatric medicine. *NPJ Genom Med.* 2016;1. pii:15012.
12. Alazami AM, Al-Qattan SM, Faqeih E, et al. Expanding the clinical and genetic heterogeneity of hereditary disorders of connective tissue. *Hum Genet.* 2016; 135:525-540.
13. Smigiel R, Kusmierska K, Pollak A, et al. Severe phenotype of De Barsy syndrome in two siblings with novel mutations in the *ALDH18A1* gene. *J Clin Med Genomics.* 2017;5:1
14. Lefebvre M, Beaufrere AM, Francannet C, et al. Extending the *ALDH18A1* clinical spectrum to severe autosomal recessive fetal cutis laxa with corpus callosum agenesis. *Am J Med Genet A.* 2018;176:2509-2512.
15. Martinelli D, Häberle J, Rubio V, et al. Understanding pyrroline-5-carboxylate synthetase deficiency: clinical, molecular, functional, and expression studies, structure-based analysis, and novel therapy with arginine. *J Inherit Metab Dis.* 2012;35:761-776.
16. Fischer-Zirnsak B, Escande-Beillard N, Ganesh J, et al. Recurrent de novo mutations affecting residue Arg138 of pyrroline-5-carboxylate synthase cause a progeroid form of autosomal-dominant cutis laxa. *Am J Hum Genet.* 2015;97:483-492.
17. Nozaki F, Kusunoki T, Okamoto N, et al. *ALDH18A1*-related cutis laxa syndrome with cyclic vomiting. *Brain Dev.* 2016;38:678-684.

18. Bholra PT, Hartley T, Bareke E, et al. Autosomal dominant cutis laxa with progeroid features due to a novel, de novo mutation in *ALDH18A1*. *J Hum Genet*. 2017;62:661-663.
19. Coutelier M, Goizet C, Durr A, et al. Alteration of ornithine metabolism leads to dominant and recessive hereditary spastic paraplegia. *Brain*. 2015;138:2191-2205.
20. Panza E, Escamilla-Honrubia JM, Marco-Marín C, et al. *ALDH18A1* gene mutations cause dominant spastic paraplegia SPG9: loss of function effect and plausibility of a dominant negative mechanism. *Brain*. 2016;139:e3.
21. Slavotinek AM, Pike M, Mills K, Hurst JA. Cataracts, motor system disorder, short stature, learning difficulties, and skeletal abnormalities: a new syndrome? *Am J Med Genet*. 1996;62:42-47.
22. Seri M, Cusano R, Forabosco P, et al. Genetic mapping to 10q23.3-q24.2, in a large Italian pedigree, of a new syndrome showing bilateral cataracts, gastroesophageal reflux, and spastic paraparesis with amyotrophy. *Am J Hum Genet*. 1999;64:586-593.
23. Kremer LS, Bader DM, Mertes C, et al. Genetic diagnosis of mendelian disorders via RNA sequencing. *Nat Commun*. 2017;8:15824.
24. Steenhof M, Kibæk M, Larsen MJ, et al. Compound heterozygous mutations in two different domains of *ALDH18A1* do not affect the amino acid levels in a patient with hereditary spastic paraplegia. *Neurogenetics*. 2018;19:145-149.
25. Koh K, Ishiura H, Beppu M, et al. Novel mutations in the *ALDH18A1* gene in complicated hereditary spastic paraplegia with cerebellar ataxia and cognitive impairment. *J Hum Genet*. 2018;63:1009-1013.

26. Magini P, Marco-Marin C, Escamilla-Honrubia JM et al. P5CS expression study in a new family with ALDH18A1-associated hereditary spastic paraplegia SPG9. *Ann Clin Transl Neurol.* 2019;6:1533-1540.
27. Wei Q, Dong HL, Pan LY et al. Clinical features and genetic spectrum in Chinese patients with recessive hereditary spastic paraplegia. *Transl Neurodegener.* 2019;8:19
28. Valle D, Simell O. The hyperornithinemias. In *The Metabolic and Molecular Bases of Inherited Disease*, 8th. ed (Scriver CR, Beaudet A L, Sly WS, Valle D, Childs B, Kinzler KW, Vogelstein B, eds.). McGraw-Hill Medical, NY. 2001, pp. 1857-1895
29. Köhler ES, Sankaranarayanan S, van Ginneken CJ et al. The human neonatal small intestine has the potential for arginine synthesis; developmental changes in the expression of arginine-synthesizing and -catabolizing enzymes. *BMC Dev Biol.* 2008;8:107.
30. van de Poll MC, Siroen MP, van Leeuwen PA et al. Interorgan amino acid exchange in humans: consequences for arginine and citrulline metabolism. *Am J Clin Nutr.* 2007;85:167-172.
31. Hu CA, Lin WW, Obie C, Valle D. Molecular enzymology of mammalian Δ^1 -pyrroline-5-carboxylate synthase. Alternative splice donor utilization generates isoforms with different sensitivity to ornithine inhibition. *J Biol Chem.* 1999; 274:6754-6762.
32. Hamano Y, Kodama H, Fujikawa Y et al. Use of immunocytochemical analysis of a duodenal biopsy specimen to identify a carrier of ornithine transcarbamylase deficiency. *N Engl J Med.* 1988;318:1521-1523.

33. Caldovic L, Morizono H, Gracia Panglao M, et al. Cloning and expression of the human N-acetylglutamate synthase gene. *Biochem Biophys Res Commun.* 2002;299:581-586.
34. Seddon AP, Zhao KY, Meister A. Activation of glutamate by gamma-glutamate kinase: formation of gamma-cis-cyclo glutamyl phosphate, an analog of gamma-glutamyl phosphate. *J Biol Chem.* 1989;264:11326-11335.
35. Phang JM, Hu CA, Valle D. Disorders of proline and hydroxyproline metabolism. In *The Metabolic and Molecular Bases of Inherited Disease*, 8th. ed (Scriver CR, Beaudet A L, Sly WS, Valle D, Childs B, Kinzler KW, Vogelstein B, eds.). McGraw-Hill Medical, NY. 2001, pp. 1821-1838.
36. Reversade B, Escande-Beillard N, Dimopoulou A, et al. Mutations in PYCR1 cause cutis laxa with progeroid features. *Nat Genet.* 2009;41:1016-1021.
37. Zaki MS, Bhat G, Sultan T, et al. PYCR2 mutations cause a lethal syndrome of microcephaly and failure to thrive. *Ann Neurol.* 2016;80:59-70.
38. Wu G, Bazer FW, Burghardt RC, et al. Proline and hydroxyproline metabolism: implications for animal and human nutrition. *Amino Acids.* 2011;40:1053-1063.
39. Kretz R, Bozorgmehr B, Kariminejad MH et al. Defect in proline synthesis: pyrroline-5-carboxylate reductase 1 deficiency leads to a complex clinical phenotype with collagen and elastin abnormalities. *J Inherit Metab Dis.* 2011;34:731-739.
40. Kardos GR, Wastyk HC, Robertson GP. Disruption of proline synthesis in melanoma inhibits protein production mediated by the GCN2 pathway. *Mol Cancer Res.* 2015;13:1408-1420.
41. Sinnige PF, van Ravenswaaij-Arts CMA, Caruso P, et al. Imaging in cutis laxa syndrome caused by a dominant negative *ALDH18A1* mutation, with hypotheses

- for intracranial vascular tortuosity and wide perivascular spaces. *Eur J Paediatr Neurol.* 2017;21:912-920.
42. Panza E, Martinelli D, Magini P et al. Hereditary spastic paraplegia is a common phenotypic finding in ARG1 deficiency, P5CS deficiency and HHH syndrome: Three inborn errors of metabolism caused by alteration of an interconnected pathway of glutamate and urea cycle metabolism. *Front Neurol.* 2019;10:131.
43. Olivieri G, Pro S, Diodato D et al. Corticospinal tract damage in HHH syndrome: a metabolic cause of hereditary spastic paraplegia. *Orphanet J Rare Dis.* 2019;14:208.
44. Pendeville H, Carpino N, Marine JC et al. The ornithine decarboxylase gene is essential for cell survival during early murine development. *Mol Cell Biol* 2001; 21, 6549-6558.
45. Phang JM. Proline metabolism in cell regulation and cancer biology: Recent advances and hypotheses. *Antioxid Redox Signal.* 2019;30:635-649.
46. Jukkola A, Kauppila S, Risteli L et al. New lethal disease involving type I and III collagen defect resembling geroderma osteodysplastica, De Barsy syndrome, and Ehlers-Danlos syndrome IV. *J Med Genet.* 1998;35:513-518.
47. Marco-Marín C, Gil-Ortiz F, Pérez-Arellano I et al. A novel two-domain architecture within the amino acid kinase enzyme family revealed by the crystal structure of *Escherichia coli* glutamate 5-kinase. *J Mol Biol.* 2007;367:1431-1446.

FIGURE LEGENDS

Figure 1. The human *ALDH18A1* gene, its protein product P5CS and the four syndromes associated with *ALDH18A1* mutations. **(A)** Linear representation of the *ALDH18A1* open reading frame, mapping to scale the different exons and superimposing on them the sites where missense mutations have been identified in *ALDH18A1*-related disorders, distinguishing the mutations occurring in each syndrome according to the key provided. **(B)** Linear representation of the P5CS polypeptide in correspondence with the open reading frame encoding it. The boundaries of the three major components (mitochondrial targeting domain, G5K and G5PR) are marked, giving residue numbers at their boundaries. The two lobes of the G5K component (based on comparison with *E. coli* G5K⁴³) are mapped and colored in different hues of green, and the three structural domains of the G5PR component (from Protein DataBank, PDB, file 2H5G; <http://www.rcsb.org/structure/2H5G>) are also mapped and are colored differentially. The two-residue deletion generated by alternative splicing (grey), and the catalytic cysteine (green) are also mapped. **(C)** Definition of the four syndromes associated to *ALDH18A1* mutations, with mapping of these mutations in the linear scheme of the P5CS polypeptide. The figures between parentheses indicate the recurrence of a given mutation in unrelated patients from different families. **(D)** Comparison of important disease traits in the four syndromes associates with *ALDH18A1* mutations, based on the clinical data for the reported patients for these syndromes.^{1-27, 41,46} Number of patients, families, mutations and genotypes for each syndrome are given on the top part. For details on the specific mutations and genotypes, see supplementary Table S1. Red hues are deeper for higher and lighter for less frequent occurrence of a disease manifestation, and reflect the mean of the percentages of patients, families and genotypes presenting a given disease trait, in a continuous linear

gradation from red (RGB scale 255/0/0/) to white (RGB scale 255/255/255). The data on age of onset and number of reported deaths in each group are not colored. Patients with intrauterine growth restriction were considered to have disease onset at birth (0 years). Differences in onset age are significant (ANOVA, $p < 0.0001$, with values for SPG9A and SPG9B groups being significantly different when mutually compared or when compared to the cutis laxa groups, $p < 0.0065$). The cell on reported deaths for ARCL3A includes one case of pregnancy interruption due to prenatal detection of multiple fetal abnormalities that were confirmed by fetal necropsy. The item on *Connective tissue weakness* is positive when any of the following traits was reported: joint laxity, pes planus, hip dislocation and/or hip dysplasia, coxa valga, inguinal hernia, genu valgum, coxa valga and mitral leak. When several traits separated by / are given for an item, the item is positive when any of these traits is present.

Figure 2. Ornithine scavenging processes (A), metabolic routes involving P5CS (B,C) and reaction catalyzed by this enzyme (D). In this figure enzymes and catalytic processes are in italic type, and the following abbreviations are used: α KT, α -ketoglutarate; ADC, arginine decarboxylase; ARG2, type 2 arginase; ASL, argininosuccinate lyase; ASS, argininosuccinate synthetase; CPS1, carbamoyl phosphate synthetase 1; GABA, γ -aminobutyric acid; GAD, glutamate decarboxylase; GDH, glutamate dehydrogenase; GLNase, glutaminase; GS, glutamine synthetase; NAG, N-acetyl-L-glutamate; NAGS, NAG synthase; OAT, ornithine ω -aminotransferase; ODC, ornithine decarboxylase; OTC, ornithine transcarbamylase; P5CDH, pyrroline-5-carboxylate dehydrogenase; P5CS, pyrroline-5-carboxylate synthetase; PYCRI,2, pyrroline-5-carboxylate reductase isoforms 1 and 2; TCA cycle, tricarboxylic acids cycle. In (A), for clarity, only the ornithine derivatives and some of the enzymes involved in the transformations shown are illustrated, with no inclusion of other

products or of ancillary substrates. In **(B, C)** P5CS is highlighted in blue, larger type, with superindices “short” and “long” denoting its two alternatively spliced forms (see the text). As in **(A)** only the intermediates that provide the carbon skeletons of the final products arginine and proline are shown, omitting for clarity other substrates or products. In **(B)** the green double-line arrow indicates activation of CPS1 by NAG, while the red blunt-ended broken double line indicates feed-back inhibition of the short form of P5CS by ornithine. The cytosolic reactions in gray are those operating in the enterocyte only until age 4-5 years²⁹. In **(C)**, where proline synthesis from glutamate and from ornithine is schematized, the possibility of making proline from imported P5C is also considered since P5C is found in blood and can enter cells.³⁵ **(D)** P5CS two-step reaction showing which component catalyzes each step. The dominance of some disease-causing mutations strongly suggests that the highly unstable glutamyl-5-phosphate formed by a subunit is used by the G5PR component of another subunit of the P5CS oligomer, as reflected in the figure.

Figure 3. Evidences that all four *ALDH18A1* P5CS syndromes involve loss-of-function of P5CS, and indications supporting a higher severity of the neurocutaneous and spastic paraplegia presentations (abbreviated, respectively, CL3 and SPG9 when dominant and recessive presentations are pooled together). **(A)** Listing of references of the published evidences that support loss of P5CS function as the disease mechanism in the four *ALDH18A1*-associated syndromes. **(B)** Frequencies of the different types of mutations found thus far in *ARCL3A* and *SPG9B*. The mutations that are most likely null as they result in truncations are marked in the key provided. *ADCL3* and *SPG9A* mutations are not shown, since they are associated exclusively with missense changes. **(C)** Box plots summarizing the ages of disease onset (left), of minimal survival (center; it corresponds to the age at last examination) and estimated disease duration (right) for patients with

the neurocutaneous syndromes (CL3) or with SPG9 syndromes. The number of patients for which these data were available or inferred from the clinical descriptions^{1-27, 41,46} are given for each bar (for age of onset data for each of the four syndromes, see Fig. 1D). Patients with intrauterine growth restriction were considered to have disease onset at birth (0 years). The box encompasses the range between the first and the third quartile, and the whiskers define the entire range. The transversal line is the median and the cross gives the mean. In all cases differences are significant (Student's t-test), with the value of p given in the figure. The onset age and maximal survival for the patients reported to have died in infancy (including an ARCL3A fetus from a pregnancy interruption because of multiple prenatal alterations) is shown with colored circles, which are full when both disease alleles were null, half-full when only one allele was null and empty when the patient hosted only missense changes. Red circles are for recessive presentations, while the blue circle is for the single patient reported to have died with a dominant presentation (ADCL3). **(D)** *In silico* assessment of disease causality by a given missense mutation (*left*) and of conservation of the residues hosting missense mutations (*right*) in these four syndromes. In the left panel the scores of the PolyPhen2 and MutPred2 servers have been added; the highest and the lowest probabilities for disease-causation would correspond to values of 2 and 0, respectively. The horizontal lines give the medians. In the right panel the ConSurf estimation of the degree of conservation of the substituted amino acid is given, with the whiskers encompassing all the values while the box encloses the 25th to 75th percentiles and the horizontal solid lines give the medians. The more negative the value the higher the conservation. The dotted line gives the mean conservation for the entire protein sequence (see legend to Table S1 for more details, and supplementary Fig. S1 for a direct illustration of conservation in aligned sequences). **(E)** Illustration of the occurrence of global

developmental delay/intellectual disability patient by patient in the four syndromes (shown on top in different grey shadows and labelled), with indication of different genotypes (dark grey, both alleles are null; lighter grey, only one null allele; the lettering code is used to differentiate the genotypes and is not explained here for brevity). Families are also identified with letters. Finally, patients are shown in alternate grey and white cells, encompassed in families. The bottom row shows positivity for the examined trait as a cross and red coloring. The asterisk marks the necropsied fetus, indicating that the trait could not be assessed in that case.

Figure 4. Rationale for the recessive and dominant effects of different P5CS mutations.

(A) Schematic explanation of why mutations that abolish protein production obligatorily give recessive inheritance while some missense mutations are recessive (right of the blue broken vertical line) and other ones (left of this line) are dominant despite their causing loss of function. **(B and C)** Mapping on the structures of the components of human P5CS, G5K **(B)** and G5PR **(C)**, of the residues found to host missense mutations in P5CS-associated syndromes (recognition code shown on the side of the figure). The G5K component structure **(B)** is a model prepared as in^{15,20} using as template the *Escherichia coli* G5K tetramer⁴³ (Protein DataBank (PDB) file 2J5T), since P5CS may be tetrameric¹⁶ and the G5K component may have a key role in forming that tetramer (see main text). Only one subunit has been colored (N- and C-lobes green and light green respectively); the ADP and L-glutamate substrates have been placed on this subunit via superimposition with the structures of bacterial G5Ks (PDB files 2AKO and 2J5T). Some loops are missing because they have no equivalent in the template bacterial protein (interruptions marked with asterisks). An external missing loop has been symbolized with a broken line, to highlight that this loop concentrates the majority of reported ADCL3 mutations. In **(C)** a part of the dimer

found in the protein crystals of the human recombinant G5PR component (PDB file 2H5G) is shown, with one subunit showing its secondary structure (cartoon representation) and having its catalytic, cofactor binding and oligomerization (truncated) domains colored pink, cyan and dark grey, respectively. The other subunit is represented in semitransparent light grey surface. For clarity, different panels are shown for mapping residues involved in amino acid substitutions in the different *ALDH18A1*-related disorders (as indicated). Note that ARCL3A mutations of both subunits (those of the subunit in surface representation are distinguished with an asterisk) cluster together in the region where the reaction takes place, as shown by the localization of the substrates, inferred by superimposition with the homologous enzymes aldehyde dehydrogenase (PDB 1AD3) and α -aminoadipate dehydrogenase (PDB 4ZUL). **(D)** Stereo view of the active center of the G5PR component to illustrate the involvement of the residues hosting ARCL3A mutations in either the interactions with the substrates or in endowing this site with proper conformation.

Figure S1. Sequences of the regions hosting the reported *ALDH18A1* missense mutations, aligned (according to ClustalW) with the corresponding regions of the P5CSs of other species or with the monofunctional microbial G5PK or G5PR (as indicated) enzymes for yeast, *E. coli*, *Thermotoga maritima* and *Burkholderia thailandensis*. Identities are highlighted in red for residues hosting ARCL3A or ADCL3 mutations and in deep blue for SPG9. Conservative replacements are highlighted cyan. The boxes above the alignments show the mutations found in each syndrome using the same color code. The three mutations found in codon 138 are listed in line, centered on residue 138. X., *Xenopus*; D., *Drosophila*; C., *Caenorhabditis*; A., *Arabidopsis*.

1
2
3
4
5
6
7
8
9
10
11
12
13
14
15
16
17
18
19
20
21
22
23
24

**Δ^1 -Pyrroline-5-carboxylate synthetase (P5CS) deficiency: An emergent
multifaceted urea cycle-related disorder.**

25
26
27
28
29
30
31
32
33
34
35
36
37
38
39
40
41
42
43
44
45
46
47
48
49
50
51
52
53
54
55
56
57
58
59
60
61
62
63
64
65

Clara Marco-Marín,^{1,2,*} Juan M. Escamilla-Honrubia,^{1,2} José L. Llácer,^{1,2} Marco Seri,^{3,4}

Emanuele Panza,³ and Vicente Rubio^{1,2,*}

Affiliations: ¹Instituto de Biomedicina de Valencia of the CSIC, Valencia, Spain;

²Centro para Investigación Biomédica en Red sobre Enfermedades Raras CIBERER-

ISCIII, Valencia, Spain; ³Department of Medical and Surgical Sciences, University of

Bologna; ⁴Medical Genetics Unit, S. Orsola-Malpighi University Hospital, Bologna,

Italy

This review was invited as a part of the JIMD issue on Ureagenesis Defects: Novel Models and Treatment Options that was the outcome of a focused meeting on this topic held in Pontresina (Switzerland) 19-21 March 2018

***Send correspondence to:**

Clara Marco-Marín and to Vicente Rubio

Instituto de Biomedicina de Valencia (IBV-CSIC) and CIBERER

C/ Jaime Roig 11. Valencia-46010, Spain

cmarco@ibv.csic.es rubio@ibv.csic.es

Phone: +34 963391760 Telefax: +34 963690800

Word count. Summary: 250 words

Text: 3901 words

Number of Figures and Tables:

Main text: 4 figures

Supplementary Material: 1 figure and 1 table

1
2
3
4
5
6
7
8
9
10
11
12
13
14
15
16
17
18
19
20
21
22
23
24
25
26
27
28
29
30
31
32
33
34
35
36
37
38
39
40
41
42
43
44
45
46
47
48
49
50
51
52
53
54
55
56
57
58
59
60
61
62
63
64
65

Summary. The bifunctional homooligomeric enzyme Δ^1 -pyrroline-5-carboxylate synthetase (P5CS) and its encoding gene *ALDH18A1* were associated with disease in 1998. Two siblings who presented paradoxical hyperammonemia (alleviated by protein), mental disability, short stature, cataracts, cutis laxa and joint laxity, were found to carry biallelic *ALDH18A1* mutations. They showed biochemical indications of decreased ornithine/proline synthesis, agreeing with the role of P5CS in the biosynthesis of these amino acids. Of 32 patients reported with this neurocutaneous syndrome, 21 familial ones hosted homozygous or compound heterozygous *ALDH18A1* mutations, while 11 sporadic ones carried *de novo* heterozygous *ALDH18A1* mutations. In 2015-2016 an upper motor neuron syndrome (spastic paraparesis/paraplegia SPG9) complicated with some traits of the neurocutaneous syndrome, although without report of cutis laxa, joint laxity or herniae, was associated with monoallelic or biallelic *ALDH18A1* mutations with, respectively, dominant and recessive inheritance. Of fifty SPG9 patients reported, 14 and 36 (34/2 familial/sporadic) carried, respectively, biallelic and monoallelic mutations. Thus, two neurocutaneous syndromes (recessive and dominant cutis laxa 3, abbreviated ARCL3A and ADCL3, respectively) and two SPG9 syndromes (recessive SPG9B and dominant SPG9A) are caused by essentially different spectra of *ALDH18A1* mutations. On the bases of the clinical data (including our own prior patients' reports), the *ALDH18A1* mutations spectra, and our knowledge on the P5CS protein, we conclude that the four syndromes share the same pathogenic mechanisms based on decreased P5CS function. Thus, these syndromes represent a continuum of increasing severity (SPG9A<SPG9B<ADCL3≤ARCL3A) of the same disease, P5CS deficiency, in which the dominant mutations cause loss-of-function by dominant-negative mechanisms.

1
2
3
4
5
6
7
8
9
10
11
12
13
14
15
16
17
18
19
20
21
22
23
24
25
26
27
28
29
30
31
32
33
34
35
36
37
38
39
40
41
42
43
44
45
46
47
48
49
50
51
52
53
54
55
56
57
58
59
60
61
62
63
64
65

Take-home message. *ALDH18A1* gene mutations causing deficiency of the *ALDH18A1*-encoded bifunctional ornithine/proline biosynthesizing enzyme P5CS result in four syndromes that represent different degrees of severity of a single disease entity, P5CS deficiency, of which two syndromes result from dominant mutations that act by dominant negative mechanisms.

Contributions of individual authors

CM-M, JE-H, EP, MS and VR conceived the study, collected literature data on the patients' clinical descriptions, systematized, analyzed and interpreted these data. CM-M, JE-H and VR made inferences on the mechanisms of inheritance based on structural reasoning and on the pathogenic mechanism by loss-of function. CM-M, JLL and VR, analyzed the consequences of the mutations on the enzyme structure and function. VR and CM-M generated the figures and wrote the manuscript, and all the authors read it and made contributions to improve its writing.

Corresponding authors: Clara Marco-Marín and Vicente Rubio

Competing interests: Clara Marco-Marín, Juan M. Escamilla-Honrubia, José L. Llácer, Marco Seri, Emanuele Panza, and Vicente Rubio declare that they have no potential conflict of interest.

Funding:

Grant of the Spanish Government (MINECO BFU2017-84264-P): “Cerrando cuentas pendientes sobre biosíntesis de arginina/urea y sus errores congénitos, y sobre regulación de nitrógeno y sus implicaciones biomédicas” (Clara Marco-Marín and Vicente Rubio). Grant of the Fundación Inocente Inocente (Vicente Rubio). Grant of American Spastic Paraplegia Foundation: ”Understanding Hereditary Spastic Paraplegia: in vivo models to identify pathogenetic mechanism and therapeutic targets for SPG9.” (Emanuele Panza)

The authors confirm independence from the sponsors; the content of the article has not been influenced by the sponsors.

Ethics approval. This work is a review and does not contain any human or animal studies performed by any of the authors. No ethical approval is needed.

Keywords. *ALDH18A1* gene-related disorders. Cutis laxa type III. Hereditary spastic paraplegia type 9. ARCL3A. ADCL3. SPG9A. SPG9B.

1. Introduction

1
2 The bifunctional enzyme Δ^1 -pyrroline 5-carboxylate synthetase (P5CS) (EC
3 1.2.1.41 & 2.7.2.11) and its encoding gene *ALDH18A1* (10q24.1) (Fig. 1A, B) were
4 associated with disease in 1998¹, when homozygous *ALDH18A1* mutations were found
5 in two siblings presenting paradoxical hyperammonemia (alleviated by protein intake),
6 mental disability, short stature, cataracts, cutis laxa, joint laxity and biochemical
7 indications of decreased ornithine and proline synthesis. Twenty one patients from 14
8 families have been reported¹⁻¹⁴ with biallelic *ALDH18A1* mutations associated to this
9 neurocutaneous syndrome called autosomal recessive cutis laxa type IIIA (ARCL3A;
10 MIM #219150) (Figs. 1C, top and 1D; Supplementary Table S1, rows in darker red
11 hue). ARCL3A usually has early onset and can be very severe, presenting cutis laxa,
12 mental disability, connective tissue weakness (joints hypermobility and dislocations, pes
13 planum, inguinal herniae) and variable degrees of progeroid facies and of intrauterine
14 and postnatal growth restriction leading to short stature. Cataracts and/or corneal
15 clouding usually occur, while failure to thrive, gastroesophageal reflux with frequent
16 vomiting, skeletal abnormalities and osteopenia are also observed (Fig. 1D). Plasma
17 levels of one or several of the four amino acids proline, arginine, citrulline and ornithine
18 can be low-normal or decreased.^{1,2-4,7,8,10}

19
20
21
22
23
24
25
26
27
28
29
30
31
32
33
34
35
36
37
38
39
40
41
42
43 In 2012 a sporadic neonatal patient was reported¹⁵ with a typical ARCL3A
44 presentation except for his hosting of a *de novo* *ALDH18A1* missense mutation together
45 with an inherited benign variant (Table S1, family 5), strongly suggesting a dominant
46 nature of the *de novo* mutation. Ten additional sporadic patients have been reported¹⁶⁻¹⁸
47 with monoallelic dominant *ALDH18A1* pathogenetic variants and cutis laxa type III
48 presentation (Fig. 1C, second panel from top, and Fig. 1D; and Table S1, rows in lighter
49 red hue) leading to the definition of ADCL3 (MIM #616603).
50
51
52
53
54
55
56
57
58
59
60
61
62
63
64
65

1
2
3
4
5
6
7
8
9
10
11
12
13
14
15
16
17
18
19
20
21
22
23
24
25
26
27
28
29
30
31
32
33
34
35
36
37
38
39
40
Greater clinical complexity became patent in 2015-2016, when heterozygous
ALDH18A1 missense mutations were associated^{19,20} with complicated spastic paraplegia
termed SPG9A (MIM #601162). Of 36 patients studied¹⁹⁻²² 34 familial cases ranged in
five families, while two cases were sporadic (Figs. 1C, bottom panel and 1D; Table S1,
light blue rows). A recessively inherited form of this motor presentation associated to
biallelic *ALDH18A1* mutations, called SPG9B (MIM # 616586) has also been found in
14 studied patients from eight families^{19,23-27} (Figs. 1C third panel from top, and Fig.1D;
Table S1, rows in darker blue). SPG9A and SPG9B are characterized by an upper motor
neuron syndrome generally of later onset, with variable degrees of weakness
(sometimes mild enough in SPG9A to be manifested, in females, only during
pregnancy, reverting afterwards²¹; pregnancy-associated initial manifestations without
postpartum reversion has also been reported in SPG9A²²), progressive spastic limb
paresis usually complicated (particularly in SPG9B²⁶) with learning disability, growth
retardation, dysmorphic features, microcephaly and/or cyclic vomiting and bilateral
cataracts, but without report of cutis laxa, joint hypermobility or herniae (Fig. 1D).
Low-normal or decreased plasma urea cycle amino acids and/or proline have been
reported in some patients^{19,20,23,24}.

41
42
43
44
45
46
47
48
49
50
51
52
53
54
55
56
57
58
59
60
61
62
63
64
65
The association with *ALDH18A1* mutations of two syndromes (neurocutaneous
and motor) having each one of them either dominant or recessive inheritance, calls for
clarification of the underlying mechanisms for this diversity. We provide here an
evidence-based unifying view founded on the concept of a disease continuum of
increasing severity in the order SPG9A<SPG9B<ADCL3≤ARCL3A corresponding to
progressively increasing loss of P5CS function, in which the dominant forms result
from loss of function due to dominant negative mechanisms.

2. P5CS: a crucial catalyst for *de novo* synthesis of ornithine and proline

1
2 Ornithine is crucial for ammonia detoxification by the urea cycle. Although not
3
4 consumed in this cycle, it is scavenged mainly by oxidation of ornithine-derived
5
6 glutamate, by conversion to putrescine or to proline, or by incorporation into body
7
8 proteins mainly as arginine (but also as ornithine-derived proline, glutamate and
9
10 glutamine) (Fig. 2A). Thus, it must be replenished by food intake (mainly as arginine)
11
12 or by *de novo* synthesis (revised in²⁸; Fig. 2B). This synthesis occurs from glutamate,
13
14 taking place in the mucosal cells of the small intestine, with subsequent conversion of
15
16 *de novo* made ornithine to either arginine (children of <5 years)²⁹ or citrulline (beyond 5
17
18 years).^{28,30} These amino acids are exported to blood, with conversion of the citrulline to
19
20 arginine by the kidney, which releases arginine to the circulation. Circulating arginine
21
22 can enter the liver and replenish decaying ornithine levels.³⁰
23
24
25
26
27

28
29 The coexistence in enterocytes' mitochondria of^{28,29,31-33} P5CS, ornithine
30
31 aminotransferase (OAT), ornithine transcarbamylase (OTC), carbamoyl phosphate
32
33 synthetase (CPS1) and the CPS1 activating enzyme N-acetyl-L-glutamate synthase
34
35 (NAGS) (Fig. 2B) strongly favors *de novo* synthesis of citrulline. Glutamate is abundant
36
37 in enterocytes and promotes ornithine synthesis by the concerted action of P5CS and
38
39 OAT, two enzymes for which glutamate is a substrate. OTC, by trapping ornithine as
40
41 citrulline using CPS1-made carbamoyl phosphate from the abundant intestinal cell
42
43 ammonia, pulls further the OAT reaction in the direction of ornithine synthesis.
44
45
46
47

48
49 Many other cell types host in their mitochondria P5CS and OAT^{28,31} (Fig. 2C).
50
51 However, unlike enterocytes, they lack NAGS, CPS1 and OTC. While in these cells
52
53 OAT is used to catabolize ornithine (as proven in OAT deficiency, which gives very
54
55 high ornithine levels²⁸), the P5CS is used to make proline *de novo* (Fig. 2C).^{2,28,31} The
56
57 P5CS polypeptide is composed of N-terminal glutamate 5-kinase (G5K) and C-terminal
58
59
60
61
62
63
64
65

1 glutamyl-5-phosphate reductase (G5PR) moieties (Fig. 1B).³¹ The P5CS oligomer
2 (believed to be a tetramer¹⁶ or hexamer²⁰) makes glutamate-5-semialdehyde (G5S) from
3 glutamate in two sequential steps (Fig. 2D). Glutamate is first phosphorylated by the
4 G5K component, using ATP. The resulting unstable³⁴ glutamyl-5-phosphate (G5P) is
5 reductively dephosphorylated to G5S in an NADPH-requiring reaction catalyzed by the
6 G5PR component (possibly of another subunit, see below). In non-intestinal cells
7 lacking OTC the unfavorable equilibrium of the OAT reaction leads to the lingering of
8 the G5S made by P5CS and to its spontaneous cyclization to Δ^1 -pyrroline-5-carboxylate
9 (P5C) (Fig. 2D).^{28,35} This last compound is reduced to proline in an NADPH-dependent
10 reaction (Fig. 2C) catalyzed by the mitochondrial Δ^1 -pyrroline-5-carboxylate
11 reductases PYCR1 and PYCR2³⁵⁻³⁷ (the letters composing the PYCR abbreviation are
12 underlined). The role of PYCR1 in proline biosynthesis is well documented,³⁶ while
13 PYCR2³⁷ may predominate functionally in the nervous system.

14 The key involvement of P5CS in the routes of *de novo* synthesis of both
15 ornithine and proline (Fig. 2B,C) is reflected in the existence of two molecular forms of
16 the P5CS polypeptide of 793 or 795 amino acids. The shorter form, resulting from the
17 skipping of codons 238 and 239 by alternative splicing³¹ (Fig. 1B), is predominantly
18 expressed in enterocytes, where it is committed to make ornithine (Fig. 2B), being
19 controlled by feed-back inhibition by ornithine.³¹ The 2-residue longer form of P5CS is
20 insensitive to ornithine and is prevalent in non-enteric cell types,^{2,31} where it is involved
21 in proline synthesis (Fig. 2C).

22 **3. *ALDH18A1*-related disorders can be manifestations of deficient production of** 23 **ornithine and proline**

24 Loss-of-function P5CS mutations should reduce or abolish *de novo* production
25 of ornithine, citrulline, arginine and proline, explaining the decreased (although
26

1 inconstantly, possibly due to blurring by food intake and tissue catabolism) plasma
2 levels of these amino acids in *ALDH18A1*-related syndromes^{1-4,7,8,10,13,15-17,19,20,23,24} (Fig.
3
4 3A). The ornithine needed for making urea can be limited in interprandial periods,
5
6 explaining the paradoxical hyperammonemia observed in the first two reported
7
8 ARCL3A patients.¹⁻³
9
10

11
12 Low proline synthesis might hamper production of the very abundant (~35% of
13
14 the body protein mass) connective tissue proteins collagen and elastin, which are
15
16 proline-rich (proline+hydroxyproline represent 25% and 14% of the mass of each of
17
18 these proteins, respectively). This likely explains (Fig. 1D) the cutis laxa and
19
20 connective tissue weakness and possibly also the bony alterations (dysmorphic features,
21
22 osteopenia,^{3,6,11,15-17} etc), the vascular tortuosity^{5,15-18}, cyclic vomiting and even cardiac
23
24 defects^{5,10,12,22} and mitral valve leaks^{19,26} observed in some of these patients. Indeed,
25
26 elastic fiber alterations have been noted in skin biopsies of patients of *ALDH18A1*-
27
28 associated syndromes.^{5-7,15} Alterations in collagen fiber bundle architecture have also
29
30 been reported.^{5,15} The corneal clouding seen in the most severe ARCL3A cases^{5,10} has
31
32 been linked to microanatomical corneal alterations affecting the extracellular matrix,
33
34 which is largely collagenous in the cornea⁵. The cataracts have been attributed² to
35
36 proline deficiency. This deficiency could restrict both protein synthesis and/or a proline-
37
38 mediated redox cycle in which P5C, which is present in the lens, is a crucial
39
40 component.²
41
42
43
44
45
46
47

48 Proline and hydroxyproline together represent about 12% of the whole body
49
50 protein mass.³⁸ Therefore, poor *de novo* synthesis of proline may be detrimental for
51
52 rapid growth in the final stages of fetal development and the first years of postnatal life
53
54 and may contribute importantly to the intrauterine and postnatal growth restriction
55
56 resulting in short stature in *ALDH18A1*-associated syndromes (Fig. 1D). The role of
57
58
59
60
61
62
63
64
65

1 proline is supported by the intrauterine growth restriction that is also observed in
2 PYCR1 deficiency,^{6,7,36,39} a proline biosynthesis disorder which does not primarily
3
4 affect ornithine synthesis. Interestingly, studies in cultured melanoma cells⁴⁰ showed
5
6 that siRNA knockdown of P5CS dramatically increased cell doubling time, apparently
7
8 because of general metabolic slowdown and inhibition of protein synthesis linked to
9
10 activation of the general control nonderepressible 2 (GCN2) protein kinase. These
11
12 effects were reversed by proline addition.
13
14
15

16 A negative impact on the mental status of subclinical chronic mild
17
18 hyperammonemia cannot be excluded in *ALDH18A1*-related disorders. However,
19
20 impaired local proline production in the nervous system may have a predominant role in
21
22 the neurocognitive alterations, since PYCR1 and PYCR2 deficiencies^{6,7,36,37,39} (two pure
23
24 disorders of proline synthesis) usually cause mental disability and even neuroanatomic
25
26 alterations (e.g. corpus callosum thinning/atrophy^{36,37,41}) found in *ALDH18A1*-related
27
28 syndromes. The mechanisms of these alterations remain to be ascertained, although
29
30 restricted protein synthesis and reduced antioxidant protection in the central nervous
31
32 system, both due to limited proline availability, might be important determinants.
33
34
35
36
37
38

39 Similarly, the pathophysiology of the upper motor neuron syndrome is
40
41 uncertain. It was proposed to be linked to ornithine¹⁹ since it was not described in
42
43 PYCR1 deficiency^{6,7,36}. Furthermore, spastic paraplegia also develops in patients of
44
45 argininemia and of hyperornithinemia-hyperammonemia-homocitrullinuria
46
47 (HHH),^{19,42,43} two syndromes in which, as in P5CS deficiency, there is mitochondrial
48
49 ornithine deficiency. It has been speculated^{42,43} that autophagy and arginine/ornithine
50
51 imbalance could be involved in causing the paraplegia manifestations. More studies are
52
53 needed to substantiate these proposals and, particularly, to link mechanistically
54
55
56
57
58
59
60
61
62
63
64
65

1
2
3
4
5
6
7
8
9
10
11
12
13
14
15
16
17
18
19
20
21
22
23
24
25
26
27
28
29
30
31
32
33
34
35
36
37
38
39
40
41
42
43
44
45
46
47
48
49
50
51
52
53
54
55
56
57
58
59
60
61
62
63
64
65

Other pathogenic possibilities remain to be explored in these syndromes, such as the potential role of polyamines (of which ornithine is a key precursor, Fig. 2A), given the crucial role of polyamines for development⁴⁴. The close metabolic relations of proline, ornithine, glutamate and glutamine (Fig. 2A,C) should also be taken into account, particularly since seizures are frequent among these patients,^{3-5,7,8,10-13,15,19,23,24,26} and given the facts that glutamate is an excitatory and potentially neurotoxic neurotransmitter while γ -aminobutyric acid (GABA) derives from glutamate and is an inhibitory neurotransmitter. A new dimension to be explored was recently open when an important signalling role of proline and its metabolism that could affect even autophagy was reported.⁴⁵

4. Two syndromes reflecting different severities of the same disease process?

We propose here that the neurocutaneous and the spastic paraplegia syndromes represent, respectively, higher and lower degrees of severity of the same disorder corresponding to higher and lower degrees of loss of P5CS function. This functional loss is reflected in the parameters listed in Fig. 3A (some of them directly reflecting P5CS activity: rows 2, 4 and 5 of this figure), of which at least some have been reported for all four syndromes. A number of observations support a greater loss of P5CS function and higher severity of the presentation in ARCL3A and ADCL3 than in SPG9 presentations: 1) null *ALDH18A1* mutations were observed more frequently in ARCL3A than in SPG9B (respectively, null/missense mutation ratios, ~1:2 and ~1:5; Figs. 1C, 3B and Table S1); 2) three patients reported with biallelic obligatory null *ALDH18A1* mutations^{5,10} presented extremely severe ARCL3A, with two dying at ≤ 6 months of age (Table S1, families 29, 31 and 35; filled red dots in the left and central panels of Fig. 3 C); 3) all ADCL3 patients were sporadic cases¹⁶⁻¹⁸ while 34 of the 36 studied SPG9A patients were familial cases¹⁹⁻²³ (Fig. 1D; Table S1, light red and light

1 blue rows), indicating that the monoallelic mutations in ADCL3 but not in SPG9A
2 caused too much disability to allow reproduction; 4) the age of disease onset was
3 earlier, survival time was higher and disease duration was longer for pooled ARCL3A
4 and ADCL3 patients than for pooled SPG9B and SPG9A patients (Fig. 3C); 5) the
5 combined scores yielded by the Polyphen2 (<http://genetics.bwh.harvard.edu/pph2>) and
6 MutPred2 (<http://mutpred.mutdb.org>) disease-causation prediction servers tended to be
7 higher for single amino acid variants found in ARCL3A and ADCL3 than for variants
8 found in SPG9 syndromes (Fig. 3D, left panel); and the scores for amino acid
9 conservation for the residues replaced in ARCL3A and ADCL3 tended to be higher than
10 for those replaced in SPG9B and SPG9A (Fig. 3D, right panel and Supplementary Fig.
11 S1) in line with the fact that higher conservation is characteristic for more important
12 residues for protein function or stability.
13
14
15
16
17
18
19
20
21
22
23
24
25
26
27

28 Fig. 1D illustrates in heat-plot style the existence of a true disease continuum for
29 the four syndromes, which share most disease traits although with different observed
30 frequencies depending on the syndrome. The most severe end of this continuum is
31 represented by the cutis laxa syndromes, and, in particular, by the three patients that
32 hosted biallelic obligatory null *ALDH18A1* mutations (Table S1, families 29, 31 and
33 35). These ARCL3A patients prove that lack of P5CS is not lethal in utero but that it
34 consistently causes very important intrauterine growth restriction leading to very low
35 birth weight (1.5, 1.8 and 1.4 kg in these three patients)^{5,10}, decreased body length and
36 head circumference.^{5,10} Other characteristic features of these three patients were
37 postnatal failure to thrive, bilateral corneal clouding (2 of the three cases^{5,10}) or very
38 early cataract (the other case¹⁰), and the occurrence of thin, wrinkled, loose and semi-
39 transparent skin with visible dermal vessels, very marked progeroid facial features, joint
40 contractures and, later on, joint luxations and/or herniae. Skin ultrastructure, studied in
41
42
43
44
45
46
47
48
49
50
51
52
53
54
55
56
57
58
59
60
61
62
63
64
65

1 one of these patients, revealed abnormal elastic fibers.¹⁰ Clearly, these three patients
2 represent the more florid and severe end of the disease continuum. At the lower severity
3 end for most manifestations are the dominant forms of SPG9, which for the traits shared
4 with the cutis laxa forms, exhibit lower frequencies of occurrence (among patients,
5 families and genotypes, Fig. 1D). A patient-by-patient exemplification of the disease
6 continuum is illustrated in Fig. 3E for global developmental delay/intellectual disability,
7 essentially constant among the ARCL3A and ADCL3 patients, also observed in all but
8 one SPG9B patient, but absent from all but one SPG9A patient.¹⁹⁻²² An exception to this
9 continuum is the lack of report of cutis laxa and of most manifestations of connective
10 tissue weakness (joint laxity/inguinal hernia; not shown separately) in SPG9A patients,
11 strongly suggesting that above a certain P5CS activity level the connective tissue
12 manifestations are either absent or are not prominent enough to be easily remarked. This
13 may be particularly so for cutis laxa, which even in the florid cases tends to ameliorate
14 with age.⁴

15
16
17
18
19
20
21
22
23
24
25
26
27
28
29
30
31
32
33
34 Concerning the upper motor neuron syndrome, it appears to be a nearly constant
35 element of all *ALDH18A1*-related syndromes, given the finding of pyramidal signs and
36 of tonus disturbance (hypotonia) in many patients with the cutis laxa syndromes. Given
37 the low age of most of these cutis laxa patients and the severity of their manifestations,
38 and since the motor syndrome appears to take time to develop, as noted for the SPG9
39 syndromes, the motor manifestations are not fully observed in most cutis laxa patients
40 or are overshadowed by the early and more severe neurocutaneous presentations
41 observed in the ARCL3A and ADCL3 syndromes. This delayed appearance of the
42 complete motor syndrome is clearly illustrated in the first two patients (brother and
43 sister) reported with ARCL3A. These patients have been followed for >10 years,
44 showing progressively more prominent motor manifestations with time despite the fact

1 that the initial manifestations were those of the neurocutaneous syndrome.¹⁻³ Thus,
2 while both patients could walk at 4 years of age, they lost the ability to walk when 12-
3
4 15 years-old as a consequence of the motor syndrome with manifestation of severe
5
6 pyramidal syndrome.³ In another ARCL3A family with four siblings of 21 to 4 years of
7
8 age,⁴ the patients, although reported in less detail, also appear to manifest the motor
9
10 syndrome after an initial cutis laxa presentation, leading to loss of ability to walk. In
11
12 fact, motor disability occurred sooner in these six ARCL3A patients^{3,4} than in most
13
14 SPG9B patients, and appeared more severe than in most SPG9A patients.
15
16
17

18
19 On the occasion of our reporting of two novel SPG9B patients, we recently
20
21 showed that SPG9B is more severe than SPG9A.²⁶ In the case of ARCL3A and
22
23 ADCL3, the patients' data suggests similar degrees of severity for these two syndromes,
24
25 as exemplified with the severe presentations observed for some ADCL3 patients
26
27 reported in detail,^{15,46} particularly a patient⁴⁶ presenting a florid clinical picture
28
29 associated with total motor disability, who died at about 3 years of age (blue circle in
30
31 Fig. 3C, middle panel). Motor disturbance was also reported for an ADCL3A patient¹⁸
32
33 who at 8 years of age was only able to walk with support. In any case, more ADCL3
34
35 patients must be identified before a sounder conclusion on differences in severity with
36
37 ARCL3A can be attained. What appears clear is that the dominant cutis laxa
38
39 presentations are more severe than SPG9 presentations and certainly much more severe
40
41 than the SPG9A presentations (Fig. 1D).
42
43
44
45
46
47
48

49 **5. Why dominant and recessive modes of inheritance?**

50
51 The clinical similarities of ARCL3A and ADCL3 agree with the operation of the
52
53 same disease mechanism for these two syndromes (different degrees of decrease in
54
55 P5CS function) irrespective of the recessive or dominant inheritance. The same can be
56
57 said for SPG9A and SPG9B. As already noted,¹⁹ the dominance cannot be attributed to
58
59
60
61
62
63
64
65

1 haploinsufficiency, since patients' parents carrying a null allele together with a wild
2 type allele are healthy (e.g.^{5,10}). A dominant negative effect appears the most plausible
3 mechanism for the dominance in ADCL3 and SPG9A^{15,16,19,20} (Fig. 4A). If P5CS is
4 functional only when in oligomeric form,^{15,16,20} the incorporation of a subunit with a
5 mutation could have a dominant negative effect if it disturbs the architecture of the
6 hybrid oligomer composed of wild-type and mutant subunits, inactivating or decreasing
7 the activity of the entire oligomer^{15,20}. This is best explained if in the normal P5CS
8 oligomer the unstable³⁴ G5P intermediate must be channelled between the G5K and
9 G5PR active centers of different subunits (Fig. 2D). The architectural defect caused by
10 the incorporation of a subunit with a dominant mutation could either prevent the
11 channelling or decrease its efficiency by altering the relations between G5K and G5PR
12 active centers of different subunits (Fig. 4A). Detailed knowledge of the P5CS
13 architecture and not only of the structures of the isolated G5K and G5PR
14 components^{15,20} (Fig. 4B,C) is needed to explain in physical terms how this channelling
15 occurs and how it can be hampered by certain mutations.
16
17
18
19
20
21
22
23
24
25
26
27
28
29
30
31
32
33
34
35

36 Only pathogenetic variants in which the mutant polypeptide is produced and is
37 soluble and integrable into the oligomer can have dominant-negative effects (Fig. 4A).
38 The formation of such hybrid mutant/wild-type oligomers was proven for dominant
39 forms found in ADCL3,¹⁶ whereas evidence for architecturally disturbed oligomers was
40 obtained for two dominant mutations found in SPG9A families.²⁰ In agreement with this
41 pathogenetic mechanism, no mutations that abolish the production of the mutant protein
42 (for example, truncating mutations) have been found in patients with the dominant
43 presentations ADCL3 or SPG9A, while these mutations have been observed in patients
44 having the recessive syndromes ARCL3A^{5,10,11,13,14} and SPG9B^{23,25} (Fig. 1C, 2B and
45 Table S1).
46
47
48
49
50
51
52
53
54
55
56
57
58
59
60
61
62
63
64
65

1
2
3
4
5
6
7
8
9
10
11
12
13
14
15
16
17
18
19
20
21
22
23
24
25
26
27
28
29
30
31
32
33
34
35
36
37
38
39
40
41
42
43
44
45
46
47
48
49
50
51
52
53
54
55
56
57
58
59
60
61
62
63
64
65

There should be complete specificity on whether a missense mutations has a recessive or a dominant negative effect. Sequence variants that cause gross misfolding, with loss of the mutant subunit, or that inactivate active centers without disturbance of intersubunit interactions should be recessive (Fig. 4A and D), whereas dominant mutations should allow integration of the mutant subunit into the oligomer, altering the architecture of the P5CS oligomer (Fig. 4A). Indeed, among the 29 missense mutations found thus far in patients with *ALDH18A1*-associated syndromes, none occurred in both a recessive syndrome and a dominant one. Only one amino acid, Arg665, was substituted in recessive and dominant SPG9, to Gln in the first case and to Leu in the second. Furthermore, mutations recurring in unrelated individuals or families always were associated with the same type of inheritance, as best exemplified for the dominant mutations affecting codon 138 in ADCL3.^{16,17}

Dominant missense mutations might also be less numerous than those causing recessive inheritance, as they can only have a dominant effect if they do not cause gross misfolding and if they affect strategic points in the protein that are involved in intersubunit interactions. Indeed, among the 29 missense mutations identified in *ALDH18A1*-associated disorders the number of recessive ones (19) nearly doubles that of dominant ones (10) (Fig. 1C and Table S1). The distribution of the mutations is also very different for recessive and dominant mutations: six of the residues affected by dominant mutations map in the G5K component of the P5CS polypeptide and only two map in the G5PR component, possibly reflecting a predominant involvement of the G5K component in intersubunit interactions in the P5CS oligomer (Fig. 1D). Interestingly, in the inferred (from bacterial G5K⁴⁷) and experimental (see²⁶) respective structural models for the G5K and G5PR components of human P5CS, the residues

involved in dominant mutations are in the surface or close to it in superficial structural elements.²⁰

The distribution of the recessive missense mutations is also different for the neurocutaneous syndrome and for the motor syndrome, as might be expected for mutations causing, correspondingly, more and less loss of P5CS function. Particularly remarkable is the clustering of missense mutations towards the C-terminus of the G5PR component in the ARCL3A syndrome. The crystal structure of the dimer of this component (Fig. 4C,D) shows that these mutations map together towards the same zone of the protein, where the interaction domain of one subunit sits between the other two domains of the G5PR component of the other subunit, at the junction of these domains, conforming the active center of the G5PR component. Although the effects of these mutations have not been determined, it is tempting to propose that all them have as their major effect the inactivation of the G5PR component. However, misfolding effects cannot be excluded, particularly for Arg765, a residue likely helping stabilize the hybrid β -sheet formed between the oligomerization domain of a subunit and the catalytic domain of the other subunit.

6. Closing remarks.

We propose here a unifying view for *ALDH18A1*-associated disorders in which 1) the clinical manifestations are due to loss of P5CS function (P5CS deficiency); 2) the different presentations conform a disease continuum of decreasing severity from the cutis laxa forms ARCL3A and ADCL3 to the motor syndromes SPG9B and SPG9A; 3) specific mutations associate with a specific syndrome because they cause different degrees of enzyme deficiency depending on the mutation; and 4) the specific recessive or dominant character of each individual mutation reflects the respective lack or

1
2
3
4
5
6
7
8
9
10
11
12
13
14
15
16
17
18
19
20
21
22
23
24
25
26
27
28
29
30
31
32
33
34
35
36
37
38
39
40
41
42
43
44
45
46
47
48
49
50
51
52
53
54
55
56
57
58
59
60
61
62
63
64
65

existence of negative effects of the mutation on the architecture of the whole enzyme oligomer.

Further evidences for this unifying view could be obtained by developing genetically modified animal models (preferably mammalian models) for each one of the four human P5CS syndromes. In turn, the determination of the structure of human P5CS could provide insight into the specific mechanisms of intramolecular channelling of the G5P intermediate that is likely to be hampered by the dominant mutations, helping predict what mutations could have a dominant-negative effect and the intensity of such effect.

ACKNOWLEDGMENTS

We thank the American Spastic Paraplegia Foundation for the EP grant "Understanding Hereditary Spastic Paraplegia: in vivo models to identify pathogenetic mechanism and therapeutic targets for SPG9". VR and CM-M were supported by grants of the Fundación Inocente Inocente and of the Spanish Government (MINECO BFU2017-84264-P).

REFERENCES

1. Kamoun P, Aral B, Saudubray JM. A new inherited metabolic disease: Δ^1 -pyrroline 5-carboxylate synthetase deficiency. *Bull Acad Natle Med.* 1998;182:131-139.
2. Baumgartner MR, Hu CA, Almashanu S, et al. Hyperammonemia with reduced ornithine, citrulline, arginine and proline: a new inborn error caused by a mutation in the gene encoding Δ^1 -pyrroline-5-carboxylate synthase. *Hum Mol Genet.* 2000;9:2853-2858.

- 1
2
3
4
5
6
7
8
9
10
11
12
13
14
15
16
17
18
19
20
21
22
23
24
25
26
27
28
29
30
31
32
33
34
35
36
37
38
39
40
41
42
43
44
45
46
47
48
49
50
51
52
53
54
55
56
57
58
59
60
61
62
63
64
65
3. Baumgartner MR, Rabier D, Nassogne MC, et al. Δ^1 -pyrroline-5-carboxylate synthase deficiency: neurodegeneration, cataracts and connective tissue manifestations combined with hyperammonaemia and reduced ornithine, citrulline, arginine and proline. *Eur J Pediatr.* 2005;164:31-36.
 4. Bicknell LS, Pitt J, Aftimos S et al. A missense mutation in *ALDH18A1*, encoding Δ^1 -pyrroline-5-carboxylate synthase (P5CS), causes an autosomal recessive neurocutaneous syndrome. *Eur J Hum Genet.* 2008;16:1176-1186.
 5. Skidmore DL, Chitayat D, Morgan T, et al. Further expansion of the phenotypic spectrum associated with mutations in *ALDH18A1*, encoding Δ^1 -pyrroline-5-carboxylate synthase (P5CS). *Am J Med Genet A.* 2011;155A:1848-1856.
 6. Zampatti S, Castori M, Fischer B, et al. De Barsy syndrome: a genetically heterogeneous autosomal recessive cutis laxa syndrome related to P5CS and PYCR1 dysfunction. *Am J Med Genet A.* 2012;158A:927-931.
 7. Gardeitchik T, Mohamed M, Fischer B, et al. Clinical and biochemical features guiding the diagnostics in neurometabolic cutis laxa. *Eur J Hum Genet.* 2014;22:888-895.
 8. Wolthuis DF, van Asbeck E, Mohamed M, et al. Cutis laxa, fat pads and retinopathy due to *ALDH18A1* mutation and review of the literature. *Eur J Paediatr Neurol.* 2014;18:511-515.
 9. Handley MT, M egarban e A, Meynert AM, et al. Loss of *ALDH18A1* function is associated with a cellular lipid droplet phenotype suggesting a link between autosomal recessive cutis laxa type 3A and Warburg Micro syndrome. *Mol Genet Genomic Med.* 2014;2:319-325.

- 1
2
3
4
5
6
7
8
9
10
11
12
13
14
15
16
17
18
19
20
21
22
23
24
25
26
27
28
29
30
31
32
33
34
35
36
37
38
39
40
41
42
43
44
45
46
47
48
49
50
51
52
53
54
55
56
57
58
59
60
61
62
63
64
65
10. Fischer B, Callewaert B, Schröter P, et al. Severe congenital cutis laxa with cardiovascular manifestations due to homozygous deletions in *ALDH18A1*. *Mol Genet Metab.* 2014;112:310-316.
 11. Stavropoulos DJ, Merico D, Jobling R, et al. Whole genome sequencing expands diagnostic utility and improves clinical management in pediatric medicine. *NPJ Genom Med.* 2016;1. pii:15012.
 12. Alazami AM, Al-Qattan SM, Faqeih E, et al. Expanding the clinical and genetic heterogeneity of hereditary disorders of connective tissue. *Hum Genet.* 2016; 135:525-540.
 13. Smigiel R, Kusmierska K, Pollak A, et al. Severe phenotype of De Barsy syndrome in two siblings with novel mutations in the *ALDH18A1* gene. *J Clin Med Genomics.* 2017;5:1
 14. Lefebvre M, Beaufriere AM, Francannet C, et al. Extending the *ALDH18A1* clinical spectrum to severe autosomal recessive fetal cutis laxa with corpus callosum agenesis. *Am J Med Genet A.* 2018;176:2509-2512.
 15. Martinelli D, Häberle J, Rubio V, et al. Understanding pyrroline-5-carboxylate synthetase deficiency: clinical, molecular, functional, and expression studies, structure-based analysis, and novel therapy with arginine. *J Inherit Metab Dis.* 2012;35:761-776.
 16. Fischer-Zirnsak B, Escande-Beillard N, Ganesh J, et al. Recurrent de novo mutations affecting residue Arg138 of pyrroline-5-carboxylate synthase cause a progeroid form of autosomal-dominant cutis laxa. *Am J Hum Genet.* 2015;97:483-492.
 17. Nozaki F, Kusunoki T, Okamoto N, et al. *ALDH18A1*-related cutis laxa syndrome with cyclic vomiting. *Brain Dev.* 2016;38:678-684.

- 1
2
3
4
5
6
7
8
9
10
11
12
13
14
15
16
17
18
19
20
21
22
23
24
25
26
27
28
29
30
31
32
33
34
35
36
37
38
39
40
41
42
43
44
45
46
47
48
49
50
51
52
53
54
55
56
57
58
59
60
61
62
63
64
65
18. Bhola PT, Hartley T, Bareke E, et al. Autosomal dominant cutis laxa with progeroid features due to a novel, de novo mutation in *ALDH18A1*. *J Hum Genet*. 2017;62:661-663.
 19. Coutelier M, Goizet C, Durr A, et al. Alteration of ornithine metabolism leads to dominant and recessive hereditary spastic paraplegia. *Brain*. 2015;138:2191-2205.
 20. Panza E, Escamilla-Honrubia JM, Marco-Marín C, et al. *ALDH18A1* gene mutations cause dominant spastic paraplegia SPG9: loss of function effect and plausibility of a dominant negative mechanism. *Brain*. 2016;139:e3.
 21. Slavotinek AM, Pike M, Mills K, Hurst JA. Cataracts, motor system disorder, short stature, learning difficulties, and skeletal abnormalities: a new syndrome? *Am J Med Genet*. 1996;62:42-47.
 22. Seri M, Cusano R, Forabosco P, et al. Genetic mapping to 10q23.3-q24.2, in a large Italian pedigree, of a new syndrome showing bilateral cataracts, gastroesophageal reflux, and spastic paraparesis with amyotrophy. *Am J Hum Genet*. 1999;64:586-593.
 23. Kremer LS, Bader DM, Mertes C, et al. Genetic diagnosis of mendelian disorders via RNA sequencing. *Nat Commun*. 2017;8:15824.
 24. Steenhof M, Kibæk M, Larsen MJ, et al. Compound heterozygous mutations in two different domains of *ALDH18A1* do not affect the amino acid levels in a patient with hereditary spastic paraplegia. *Neurogenetics*. 2018;19:145-149.
 25. Koh K, Ishiura H, Beppu M, et al. Novel mutations in the *ALDH18A1* gene in complicated hereditary spastic paraplegia with cerebellar ataxia and cognitive impairment. *J Hum Genet*. 2018;63:1009-1013.

- 1
2
3
4
5
6
7
8
9
10
11
12
13
14
15
16
17
18
19
20
21
22
23
24
25
26
27
28
29
30
31
32
33
34
35
36
37
38
39
40
41
42
43
44
45
46
47
48
49
50
51
52
53
54
55
56
57
58
59
60
61
62
63
64
65
26. Magini P, Marco-Marin C, Escamilla-Honrubia JM et al. P5CS expression study in a new family with ALDH18A1-associated hereditary spastic paraplegia SPG9. *Ann Clin Transl Neurol.* 2019;6:1533-1540.
27. Wei Q, Dong HL, Pan LY et al. Clinical features and genetic spectrum in Chinese patients with recessive hereditary spastic paraplegia. *Transl Neurodegener.* 2019;8:19
28. Valle D, Simell O. The hyperornithinemias. In *The Metabolic and Molecular Bases of Inherited Disease*, 8th. ed (Scriver CR, Beaudet A L, Sly WS, Valle D, Childs B, Kinzler KW, Vogelstein B, eds.). McGraw-Hill Medical, NY. 2001, pp. 1857-1895
29. Köhler ES, Sankaranarayanan S, van Ginneken CJ et al. The human neonatal small intestine has the potential for arginine synthesis; developmental changes in the expression of arginine-synthesizing and -catabolizing enzymes. *BMC Dev Biol.* 2008;8:107.
30. van de Poll MC, Siroen MP, van Leeuwen PA et al. Interorgan amino acid exchange in humans: consequences for arginine and citrulline metabolism. *Am J Clin Nutr.* 2007;85:167-172.
31. Hu CA, Lin WW, Obie C, Valle D. Molecular enzymology of mammalian Δ^1 -pyrroline-5-carboxylate synthase. Alternative splice donor utilization generates isoforms with different sensitivity to ornithine inhibition. *J Biol Chem.* 1999; 274:6754-6762.
32. Hamano Y, Kodama H, Fujikawa Y et al. Use of immunocytochemical analysis of a duodenal biopsy specimen to identify a carrier of ornithine transcarbamylase deficiency. *N Engl J Med.* 1988;318:1521-1523.

- 1
2
3
4
5
6
7
8
9
10
11
12
13
14
15
16
17
18
19
20
21
22
23
24
25
26
27
28
29
30
31
32
33
34
35
36
37
38
39
40
41
42
43
44
45
46
47
48
49
50
51
52
53
54
55
56
57
58
59
60
61
62
63
64
65
33. Caldovic L, Morizono H, Gracia Panglao M, et al. Cloning and expression of the human N-acetylglutamate synthase gene. *Biochem Biophys Res Commun.* 2002;299:581-586.
34. Seddon AP, Zhao KY, Meister A. Activation of glutamate by gamma-glutamate kinase: formation of gamma-cis-cycloglutamyl phosphate, an analog of gamma-glutamyl phosphate. *J Biol Chem.* 1989;264:11326-11335.
35. Phang JM, Hu CA, Valle D. Disorders of proline and hydroxyproline metabolism. In *The Metabolic and Molecular Bases of Inherited Disease*, 8th. ed (Scriver CR, Beaudet A L, Sly WS, Valle D, Childs B, Kinzler KW, Vogelstein B, eds.). McGraw-Hill Medical, NY. 2001, pp. 1821-1838.
36. Reversade B, Escande-Beillard N, Dimopoulou A, et al. Mutations in PYCR1 cause cutis laxa with progeroid features. *Nat Genet.* 2009;41:1016-1021.
37. Zaki MS, Bhat G, Sultan T, et al. PYCR2 mutations cause a lethal syndrome of microcephaly and failure to thrive. *Ann Neurol.* 2016;80:59-70.
38. Wu G, Bazer FW, Burghardt RC, et al. Proline and hydroxyproline metabolism: implications for animal and human nutrition. *Amino Acids.* 2011;40:1053-1063.
39. Kretz R, Bozorgmehr B, Kariminejad MH et al. Defect in proline synthesis: pyrroline-5-carboxylate reductase 1 deficiency leads to a complex clinical phenotype with collagen and elastin abnormalities. *J Inherit Metab Dis.* 2011;34:731-739.
40. Kardos GR, Wastyk HC, Robertson GP. Disruption of proline synthesis in melanoma inhibits protein production mediated by the GCN2 pathway. *Mol Cancer Res.* 2015;13:1408-1420.
41. Sinnige PF, van Ravenswaaij-Arts CMA, Caruso P, et al. Imaging in cutis laxa syndrome caused by a dominant negative *ALDH18A1* mutation, with hypotheses

1
2
3
4
5
6
7
8
9
10
11
12
13
14
15
16
17
18
19
20
21
22
23
24
25
26
27
28
29
30
31
32
33
34
35
36
37
38
39
40
41
42
43
44
45
46
47
48
49
50
51
52
53
54
55
56
57
58
59
60
61
62
63
64
65

for intracranial vascular tortuosity and wide perivascular spaces. *Eur J Paediatr Neurol.* 2017;21:912-920.

42. Panza E, Martinelli D, Magini P et al. Hereditary spastic paraplegia is a common phenotypic finding in ARG1 deficiency, P5CS deficiency and HHH syndrome: Three inborn errors of metabolism caused by alteration of an interconnected pathway of glutamate and urea cycle metabolism. *Front Neurol.* 2019;10:131.
43. Olivieri G, Pro S, Diodato D et al. Corticospinal tract damage in HHH syndrome: a metabolic cause of hereditary spastic paraplegia. *Orphanet J Rare Dis.* 2019;14:208.
44. Pendeville H, Carpino N, Marine JC et al. The ornithine decarboxylase gene is essential for cell survival during early murine development. *Mol Cell Biol* 2001; 21, 6549-6558.
45. Phang JM. Proline metabolism in cell regulation and cancer biology: Recent advances and hypotheses. *Antioxid Redox Signal.* 2019;30:635-649.
46. Jukkola A, Kauppila S, Risteli L et al. New lethal disease involving type I and III collagen defect resembling geroderma osteodysplastica, De Barsy syndrome, and Ehlers-Danlos syndrome IV. *J Med Genet.* 1998;35:513-518.
47. Marco-Marín C, Gil-Ortiz F, Pérez-Arellano I et al. A novel two-domain architecture within the amino acid kinase enzyme family revealed by the crystal structure of *Escherichia coli* glutamate 5-kinase. *J Mol Biol.* 2007;367:1431-1446.

FIGURE LEGENDS

1
2 **Figure 1.** The human *ALDH18A1* gene, its protein product P5CS and the four
3
4 syndromes associated with *ALDH18A1* mutations. **(A)** Linear representation of the
5
6 *ALDH18A1* open reading frame, mapping to scale the different exons and
7
8 superimposing on them the sites where missense mutations have been identified in
9
10 *ALDH18A1*-related disorders, distinguishing the mutations occurring in each syndrome
11
12 according to the key provided. **(B)** Linear representation of the P5CS polypeptide in
13
14 correspondence with the open reading frame encoding it. The boundaries of the three
15
16 major components (mitochondrial targeting domain, G5K and G5PR) are marked,
17
18 giving residue numbers at their boundaries. The two lobes of the G5K component
19
20 (based on comparison with *E. coli* G5K⁴³) are mapped and colored in different hues of
21
22 green, and the three structural domains of the G5PR component (from Protein
23
24 DataBank, PDB, file 2H5G; <http://www.rcsb.org/structure/2H5G>) are also mapped and
25
26 are colored differentially. The two-residue deletion generated by alternative splicing
27
28 (grey), and the catalytic cysteine (green) are also mapped. **(C)** Definition of the four
29
30 syndromes associated to *ALDH18A1* mutations, with mapping of these mutations in the
31
32 linear scheme of the P5CS polypeptide. The figures between parentheses indicate the
33
34 recurrence of a given mutation in unrelated patients from different families. **(D)**
35
36 Comparison of important disease traits in the four syndromes associates with
37
38 *ALDH18A1* mutations, based on the clinical data for the reported patients for these
39
40 syndromes.^{1-27, 41,46} Number of patients, families, mutations and genotypes for each
41
42 syndrome are given on the top part. For details on the specific mutations and genotypes,
43
44 see supplementary Table S1. Red hues are deeper for higher and lighter for less frequent
45
46 occurrence of a disease manifestation, and reflect the mean of the percentages of
47
48 patients, families and genotypes presenting a given disease trait, in a continuous linear
49
50
51
52
53
54
55
56
57
58
59
60
61
62
63
64
65

1 gradation from red (RGB scale 255/0/0/) to white (RGB scale 255/255/255). The data
2 on age of onset and number of reported deaths in each group are not colored. Patients
3 with intrauterine growth restriction were considered to have disease onset at birth (0
4 years). Differences in onset age are significant (ANOVA, $p < 0.0001$, with values for
5 SPG9A an SPG9B groups being significantly different when mutually compared or
6 when compared to the cutis laxa groups, $p < 0.0065$). The cell on reported deaths for
7 ARCL3A includes one case of pregnancy interruption due to prenatal detection of
8 multiple fetal abnormalities that were confirmed by fetal necropsy. The item on
9 *Connective tissue weakness* is positive when any of the following traits was reported:
10 joint laxity, pes planus, hip dislocation and/or hip dysplasia, coxa valga, inguinal hernia,
11 genu valgum, coxa valga and mitral leak. When several traits separated by / are given
12 for an item, the item is positive when any of these traits is present.

13
14
15
16
17
18
19
20
21
22
23
24
25
26
27
28
29
30 **Figure 2.** Ornithine scavenging processes (A), metabolic routes involving P5CS (B,C)
31 and reaction catalyzed by this enzyme (D). In this figure enzymes and catalytic
32 processes are in italic type, and the following abbreviations are used: α KT, α -
33 ketoglutarate; *ADC*, arginine decarboxylase; *ARG2*, type 2 arginase; *ASL*,
34 argininosuccinate lyase; *ASS*, argininosuccinate synthetase; *CPS1*, carbamoyl phosphate
35 synthetase 1; *GABA*, γ -aminobutyric acid; *GAD*, glutamate decarboxylase; *GDH*,
36 glutamate dehydrogenase; *GLNase*, glutaminase; *GS*, glutamine synthetase; *NAG*, N-
37 acetyl-L-glutamate; *NAGS*, NAG synthase; *OAT*, ornithine ω -aminotransferase; *ODC*,
38 ornithine decarboxylase; *OTC*, ornithine transcarbamylase; *P5CDH*, pyrroline-5-
39 carboxylate dehydrogenase; *P5CS*, pyrroline-5-carboxylate synthetase; *PYCR1,2*,
40 pyrroline-5-carboxylate reductase isoforms 1 and 2; *TCA cycle*, tricarboxylic acids
41 cycle. In (A), for clarity, only the ornithine derivatives and some of the enzymes
42 involved in the transformations shown are illustrated, with no inclusion of other
43
44
45
46
47
48
49
50
51
52
53
54
55
56
57
58
59
60
61
62
63
64
65

1 products or of ancillary substrates. In **(B, C)** P5CS is highlighted in blue, larger type,
2 with superindices “short” and “long” denoting its two alternatively spliced forms (see
3 the text). As in **(A)** only the intermediates that provide the carbon skeletons of the final
4 products arginine and proline are shown, omitting for clarity other substrates or
5 products. In **(B)** the green double-line arrow indicates activation of CPS1 by NAG,
6 while the red blunt-ended broken double line indicates feed-back inhibition of the short
7 form of P5CS by ornithine. The cytosolic reactions in gray are those operating in the
8 enterocyte only until age 4-5 years²⁹. In **(C)**, where proline synthesis from glutamate
9 and from ornithine is schematized, the possibility of making proline from imported P5C
10 is also considered since P5C is found in blood and can enter cells.³⁵ **(D)** P5CS two-step
11 reaction showing which component catalyzes each step. The dominance of some
12 disease-causing mutations strongly suggests that the highly unstable glutamyl-5-
13 phosphate formed by a subunit is used by the G5PR component of another subunit of
14 the P5CS oligomer, as reflected in the figure.

15
16
17
18
19
20
21
22
23
24
25
26
27
28
29
30
31
32
33
34
35 **Figure 3.** Evidences that all four *ALDH18A1* P5CS syndromes involve loss-of-function
36 of P5CS, and indications supporting a higher severity of the neurocutaneous and spastic
37 paraplegia presentations (abbreviated, respectively, CL3 and SPG9 when dominant and
38 recessive presentations are pooled together). **(A)** Listing of references of the published
39 evidences that support loss of P5CS function as the disease mechanism in the four
40 *ALDH18A1*-associated syndromes. **(B)** Frequencies of the different types of mutations
41 found thus far in ARCL3A and SPG9B. The mutations that are most likely null as they
42 result in truncations are marked in the key provided. ADCL3 and SPG9A mutations are
43 not shown, since they are associated exclusively with missense changes. **(C)** Box plots
44 summarizing the ages of disease onset (left), of minimal survival (center; it corresponds
45 to the age at last examination) and estimated disease duration (right) for patients with
46
47
48
49
50
51
52
53
54
55
56
57
58
59
60
61
62
63
64
65

1 the neurocutaneous syndromes (CL3) or with SPG9 syndromes. The number of patients
2 for which these data were available or inferred from the clinical descriptions^{1-27, 41,46} are
3 given for each bar (for age of onset data for each of the four syndromes, see Fig. 1D).
4
5 Patients with intrauterine growth restriction were considered to have disease onset at
6 birth (0 years). The box encompasses the range between the first and the third quartile,
7 and the whiskers define the entire range. The transversal line is the median and the cross
8 gives the mean. In all cases differences are significant (Student's t-test), with the value
9 of p given in the figure. The onset age and maximal survival for the patients reported to
10 have died in infancy (including an ARCL3A fetus from a pregnancy interruption
11 because of multiple prenatal alterations) is shown with colored circles, which are full
12 when both disease alleles were null, half-full when only one allele was null and empty
13 when the patient hosted only missense changes. Red circles are for recessive
14 presentations, while the blue circle is for the single patient reported to have died with a
15 dominant presentation (ADCL3). **(D)** *In silico* assessment of disease causality by a
16 given missense mutation (*left*) and of conservation of the residues hosting missense
17 mutations (*right*) in these four syndromes. In the left panel the scores of the PolyPhen2
18 and MutPred2 servers have been added; the highest and the lowest probabilities for
19 disease-causation would correspond to values of 2 and 0, respectively. The horizontal
20 lines give the medians. In the right panel the ConSurf estimation of the degree of
21 conservation of the substituted amino acid is given, with the whiskers encompassing all
22 the values while the box encloses the 25th to 75th percentiles and the horizontal solid
23 lines give the medians. The more negative the value the higher the conservation. The
24 dotted line gives the mean conservation for the entire protein sequence (see legend to
25 Table S1 for more details, and supplementary Fig. S1 for a direct illustration of
26 conservation in aligned sequences). **(E)** Illustration of the occurrence of global
27
28
29
30
31
32
33
34
35
36
37
38
39
40
41
42
43
44
45
46
47
48
49
50
51
52
53
54
55
56
57
58
59
60
61
62
63
64
65

1 developmental delay/intellectual disability patient by patient in the four syndromes
2 (shown on top in different grey shadows and labelled), with indication of different
3
4 genotypes (dark grey, both alleles are null; lighter grey, only one null allele; the
5
6 lettering code is used to differentiate the genotypes and is not explained here for
7
8 brevity). Families are also identified with letters. Finally, patients are shown in alternate
9
10 grey and white cells, encompassed in families. The bottom row shows positivity for the
11
12 examined trait as a cross and red coloring. The asterisk marks the necropsied fetus,
13
14 indicating that the trait could not be assessed in that case.
15
16
17
18
19

20 **Figure 4.** Rationale for the recessive and dominant effects of different P5CS mutations.

21
22 **(A)** Schematic explanation of why mutations that abolish protein production
23
24 obligatorily give recessive inheritance while some missense mutations are recessive
25
26 (right of the blue broken vertical line) and other ones (left of this line) are dominant
27
28 despite their causing loss of function. **(B and C)** Mapping on the structures of the
29
30 components of human P5CS, G5K **(B)** and G5PR **(C)**, of the residues found to host
31
32 missense mutations in P5CS-associated syndromes (recognition code shown on the side
33
34 of the figure). The G5K component structure **(B)** is a model prepared as in^{15,20} using as
35
36 template the *Escherichia coli* G5K tetramer⁴³ (Protein DataBank (PDB) file 2J5T),
37
38 since P5CS may be tetrameric¹⁶ and the G5K component may have a key role in
39
40 forming that tetramer (see main text). Only one subunit has been colored (N- and C-
41
42 lobes green and light green respectively); the ADP and L-glutamate substrates have
43
44 been placed on this subunit via superimposition with the structures of bacterial G5Ks
45
46 (PDB files 2AKO and 2J5T). Some loops are missing because they have no equivalent
47
48 in the template bacterial protein (interruptions marked with asterisks). An external
49
50 missing loop has been symbolized with a broken line, to highlight that this loop
51
52 concentrates the majority of reported ADCL3 mutations. In **(C)** a part of the dimer
53
54
55
56
57
58
59
60
61
62
63
64
65

1 found in the protein crystals of the human recombinant G5PR component (PDB file
2 2H5G) is shown, with one subunit showing its secondary structure (cartoon
3 representation) and having its catalytic, cofactor binding and oligomerization
4 (truncated) domains colored pink, cyan and dark grey, respectively. The other subunit is
5 represented in semitransparent light grey surface. For clarity, different panels are shown
6 for mapping residues involved in amino acid substitutions in the different *ALDH18A1*-
7 related disorders (as indicated). Note that ARCL3A mutations of both subunits (those of
8 the subunit in surface representation are distinguished with an asterisk) cluster together
9 in the region where the reaction takes place, as shown by the localization of the
10 substrates, inferred by superimposition with the homologous enzymes aldehyde
11 dehydrogenase (PDB 1AD3) and α -aminoadipate dehydrogenase (PDB 4ZUL). (D)
12 Stereo view of the active center of the G5PR component to illustrate the involvement of
13 the residues hosting ARCL3A mutations in either the interactions with the substrates or
14 in endowing this site with proper conformation.

15
16
17
18
19
20
21
22
23
24
25
26
27
28
29
30
31
32
33
34
35 **Figure S1.** Sequences of the regions hosting the reported *ALDH18A1* missense
36 mutations, aligned (according to ClustalW) with the corresponding regions of the
37 P5CSs of other species or with the monofunctional microbial G5PK or G5PR (as
38 indicated) enzymes for yeast, *E. coli*, *Thermotoga maritima* and *Burkholderia*
39 *thailandensis*. Identities are highlighted in red for residues hosting ARCL3A or ADCL3
40 mutations and in deep blue for SPG9. Conservative replacements are highlighted cyan.
41 The boxes above the alignments show the mutations found in each syndrome using the
42 same color code. The three mutations found in codon 138 are listed in line, centered on
43 residue 138. X., *Xenopus*; D., *Drosophila*; C., *Caenorhabditis*; A., *Arabidopsis*.

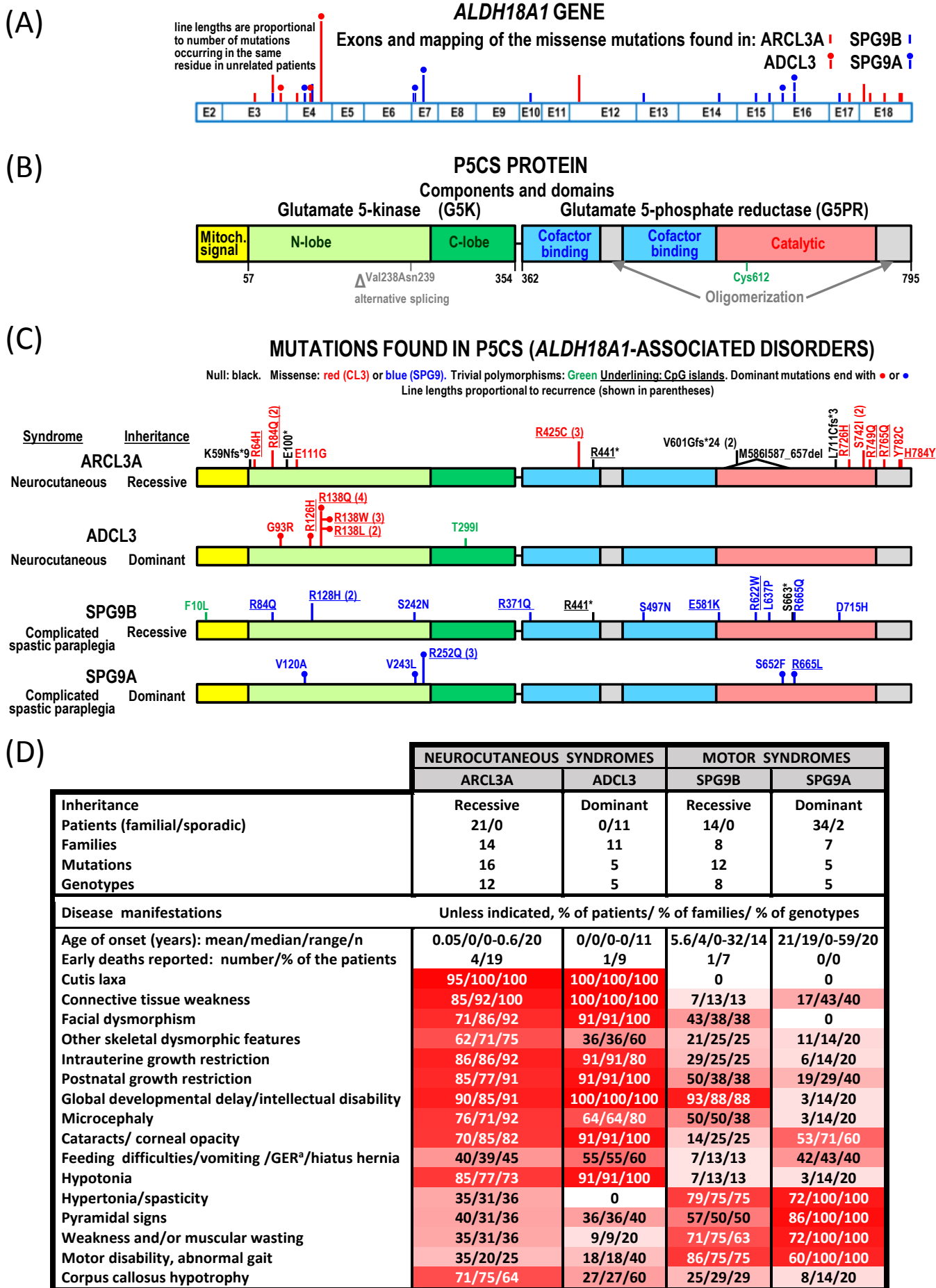
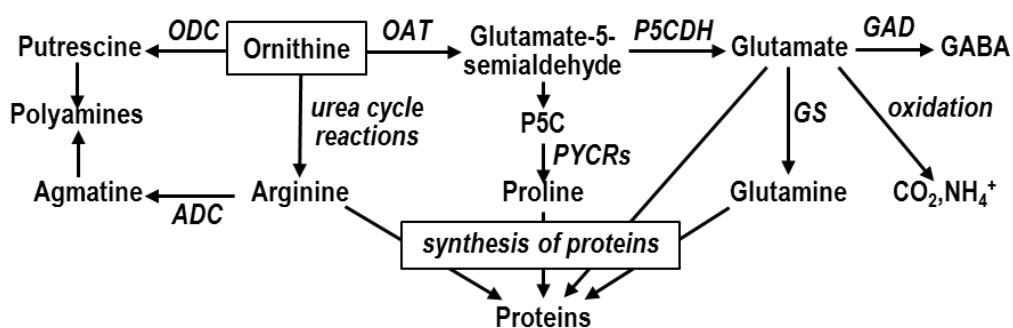


Figure 1

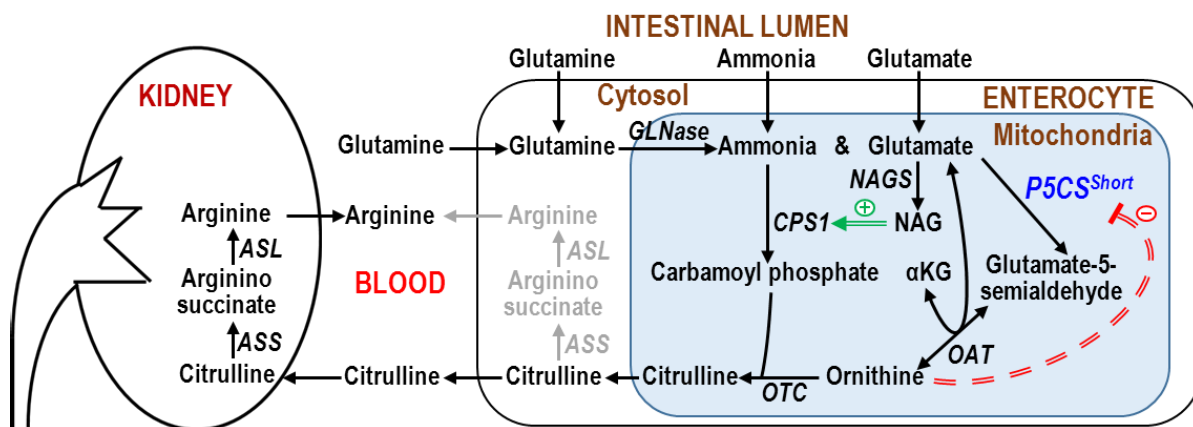
(A)

PROCESSES THAT CONSUME ORNITHINE



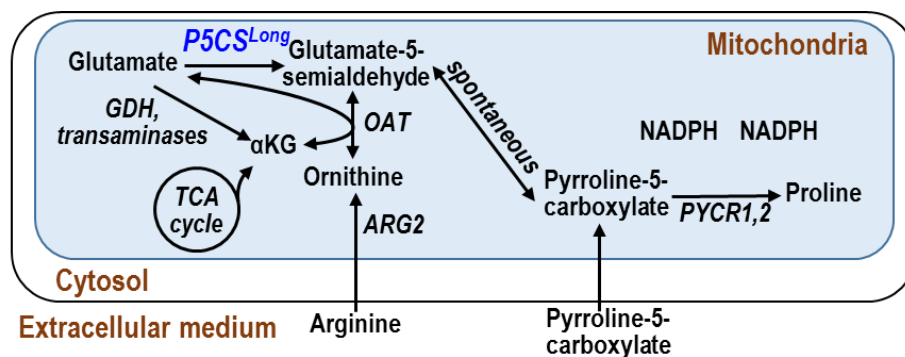
(B)

P5CS AND ORNITHINE SYNTHESIS



(C)

P5CS AND PROLINE SYNTHESIS



(D)

P5CS REACTION

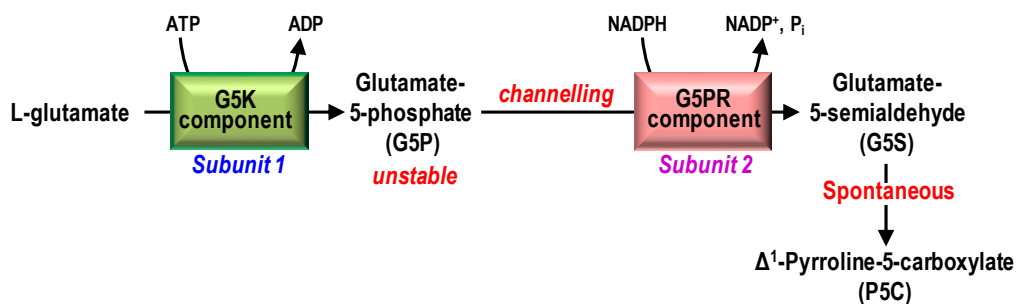


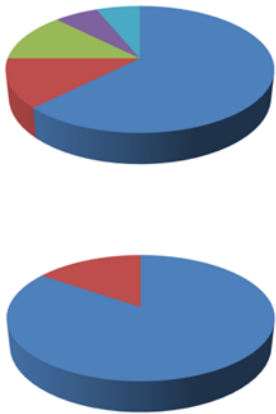
Figure 2

(A)

REFERENCES REPORTING THE EVIDENCES FOR P5CS FUNCTION LOSS IN <i>ALDH18A1</i> SYNDROMES				
	ARCL3A	ADCL3	SPG9B	SPG9A
Low-normal/ decreased plasma levels of Pro/Arg/Orn/Cit (at least one)	1-4, 7, 8, 10, 13	15-17	23, 24	19, 20
Decreased Glu→Pro flow in cultured patient-derived or transformed cells	1, 2	16	NT	19
Proline requirement for growth of patient fibroblasts or of mutant <i>ALDH18A1</i> -transformed cells	2	NT	23	NT
Decreased P5CS protein level in patient fibroblasts or in mutant <i>ALDH18A1</i> -transformed cells	2, 5, 9, 10, 20, 23	15	23	20
Decreased specific activity of recombinantly produced and purified mutant P5CS enzyme	NT	NT	20	26
Loss or substitution of catalytic or substrate-binding residues in the P5CS mutant	4-8, 10, 11, 13, 14	--	23, 25	19, 20

NT = not tested

(B)

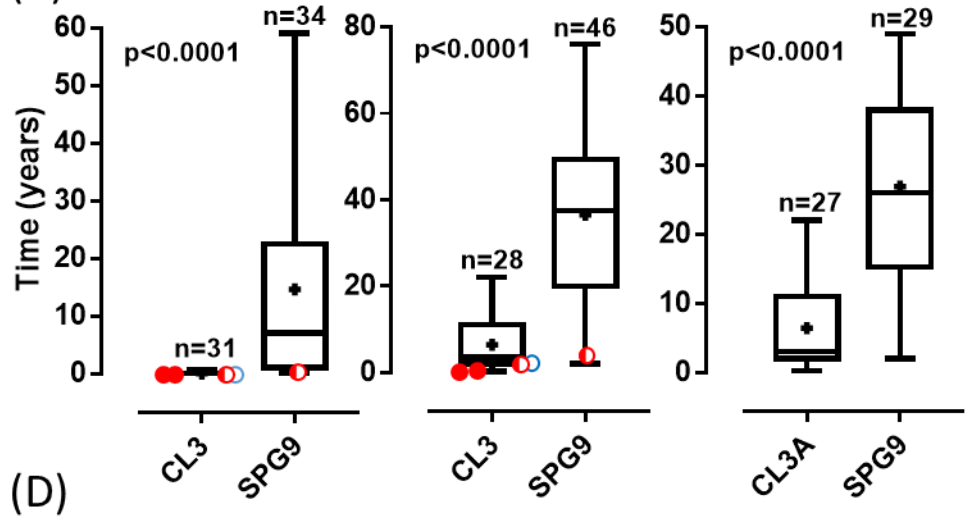


Mutation type

- Missense
- Nonsense
- Small deletions
- Large deletions
- Splicing

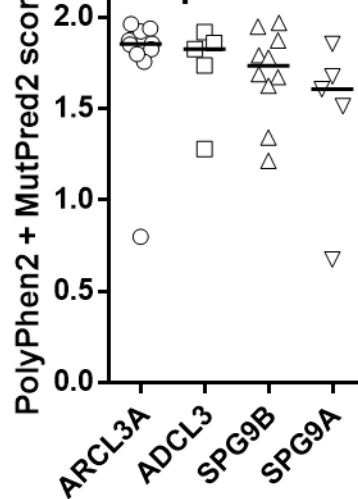
Null

(C) Age of onset Minimal survival Disease duration

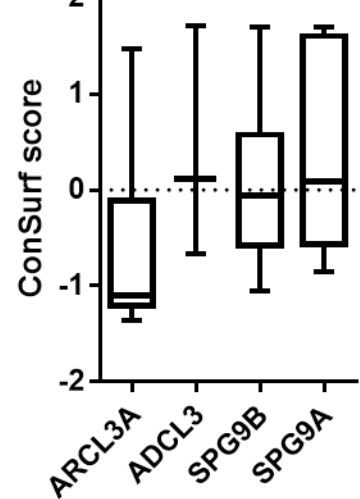


(D)

Pathogenicity prediction



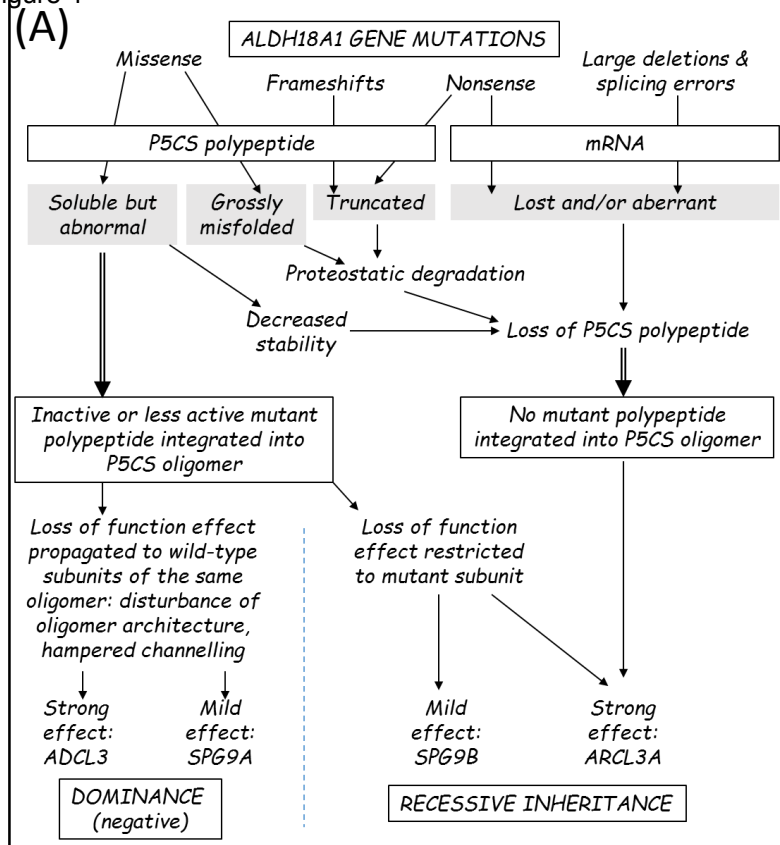
Amino acid conservation



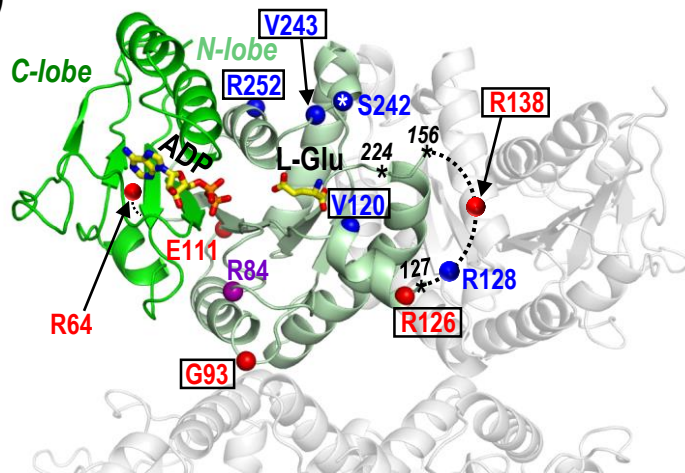
(E)

Syndrome	ARCL3A										ADCL3										SPG9B										SPG9A																					
Genotype	0	A	E	B	J	K	G	F	X	α	N	P	R	S	T	C	D	H	I	L	M	Q	W	O	U	V	Y	Z	V	W	X	Y	Z																			
Family	C	F	G	L	M	N	E	B	J	A	K	D	I	H	a	k	b	c	d	e	f	g	h	i	j	Q	S	T	O	α	R	P	U	V	W	X	Y	Z	X	Y	Z	Y	Z									
Patient	*	*	*	*	*	*	*	*	*	*	*	*	*	*	*	*	*	*	*	*	*	*	*	*	*	*	*	*	*	*	*	*	*	*	*	*	*	*	*	*	*	*	*	*	*	*	*	*	*	*	*	*

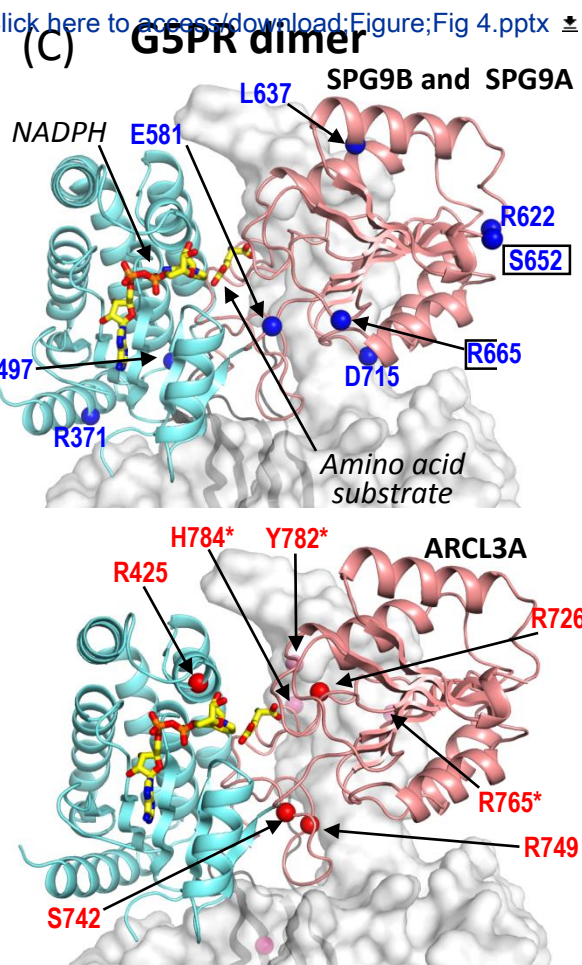
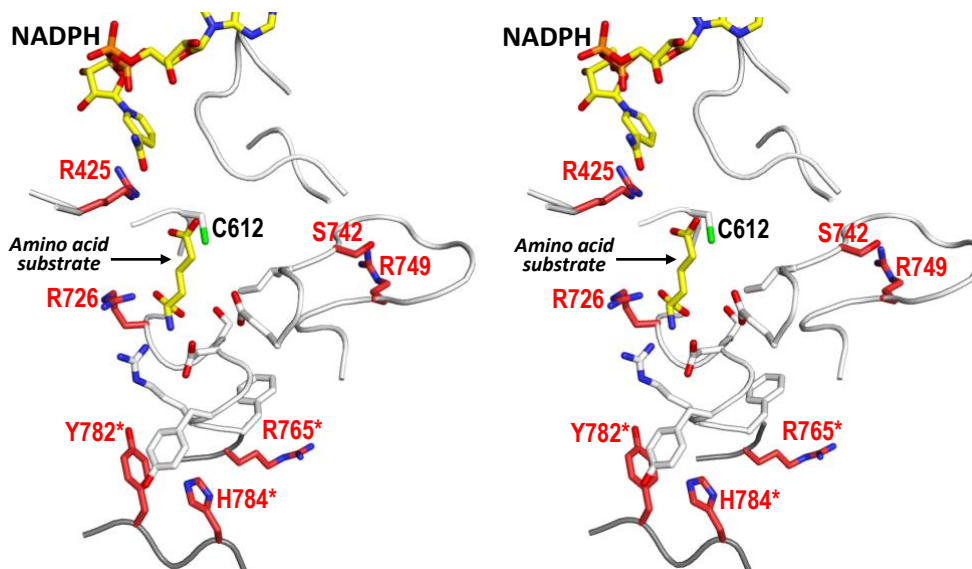
Figure 3



(B) Model of G5K tetramer



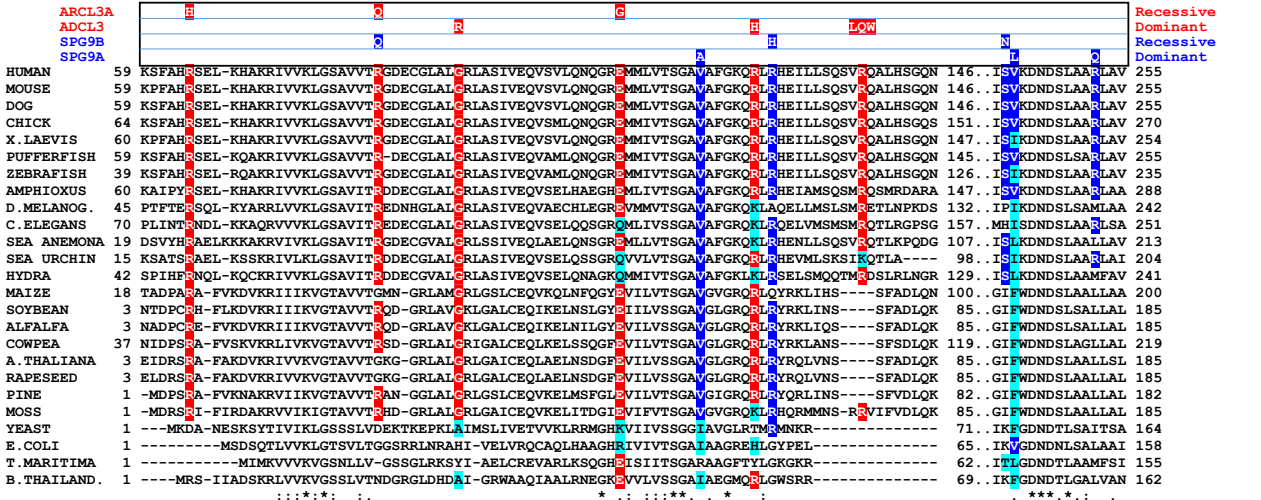
(D)



Residues found mutated in:

ARCL3A: Red ADCL3: Red
 SPG9B: Blue SPG9A: Blue
 Both ARCL3A and SPG9B: Purple

G5K COMPONENT
Missense mutations classified per clinical form



G5PR COMPONENT
Missense mutations classified per clinical form

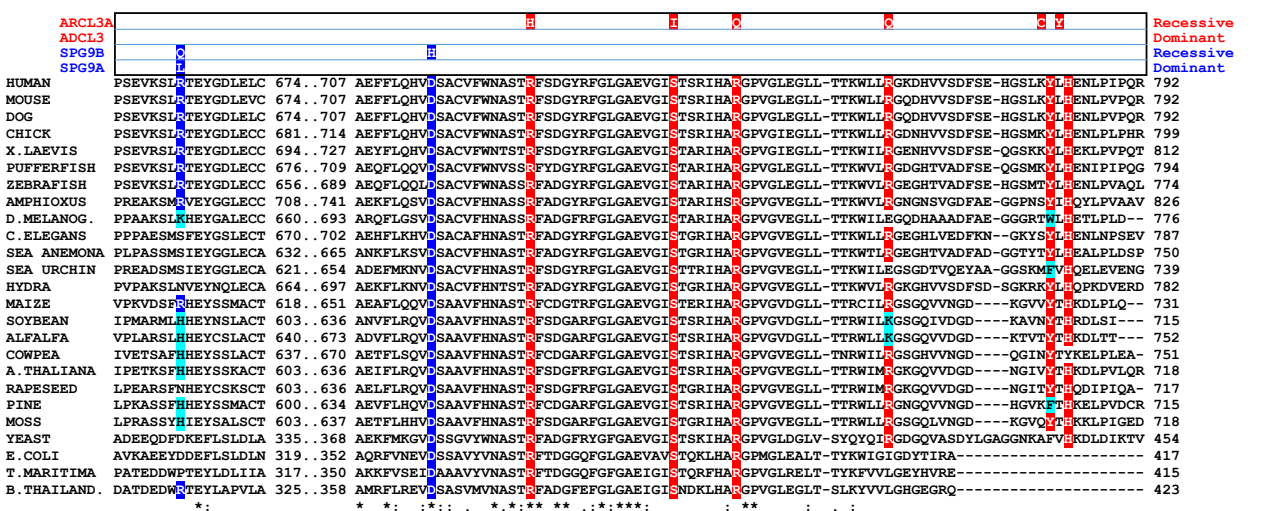
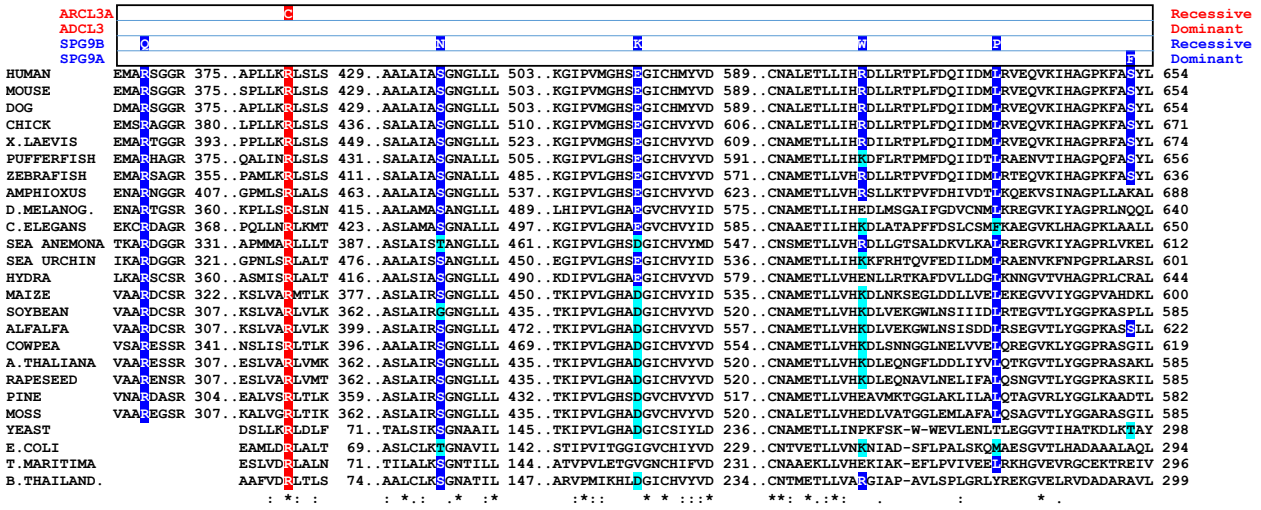


Figure S1. Sequences of the regions hosting the reported ALDH18A1 missense mutations aligned (according to ClustalW) with the corresponding regions of the P5CSs of other species or with the monofunctional microbial G5PK or G5PR (as indicated) for yeast, *E. coli*, *Thermotoga maritima* and *Burkholderia thailandensis*. Identities are highlighted in red for residues hosting ARCL3A or ADCL3 mutations and in deep blue for SPG9. Conservative replacements are highlighted cyan. The boxes above the alignments show the mutations found in each column using the same color code. The three mutations found in codon 138 are listed in line, centered on residue 138. X., *Xenopus*; D., *Drosophila*; C., *Caenorhabditis*; A. *Arabidopsis*.

Supplementary Table S1. Mutations, genotypes and predicted and observed disease severity and effects in patients and families with *ALDH18A1*-related genetic disorders.

Family # /number of patients ^a	Mutant alleles (nucleotide change) ^b	E/T ^c	Protein changes ^d	P5CS component % Component loss in truncations ^e	Syndrome ^f	Pathogenicity server prediction				Conservation		Clinical severity (0-10) ^l	Inferred severity of missense mutation ^m	P5CS-related data ⁿ
						Polyphen 2 ^g		MutPred2 Score ^h	Mutation taster ⁱ	Base PhyloP score ^j	Amino acid ConSurf score ^k			
						Prediction	Score							
1/1 ¹¹	<i>c.191G>A</i>	E3	p.(R64H)	G5K	ARCL3A	Prob.damaging	0.999	0.856	Dis.-causing	5.17	-1.36	9	VS	
	<i>c.1321C>T</i>	E12	p.(R441*)	80% G5PR		NA	NA	NA	Dis.-causing	3.63				
2/2 ¹⁻³ 3/1 ¹²	<i>c.251G>A</i> (homozygous)	E3	p.(R84Q) (homozygous)	G5K	ARCL3A	Prob. damaging	0.997	0.875	Dis.-causing	5.17	0.05	7	S	↓↓ growth of transformed CHO cells if Pro not added. Long P5CS ^{R84Q} unstable. ² ↓Glu-to-Pro flow in patient fibroblasts ³
4/1 ²⁴	<i>c.251G>A</i>	E3	p.(R84Q)	G5K	SPG9B	Prob.damaging	0.997	0.875	Dis.-causing	5.17	0.05	5		
	<i>c.1741G>A</i>	E14	p.(E581K)	G5PR		Prob.damaging	0.954	0.824	Dis.-causing	3.65	-0.17		I	G5PR active site residue
5/1 sporadic ¹⁵	<i>c.277G>A</i>	E3	p.(G93R)	G5K	ADCL3	Prob.damaging	1.000	0.918	Dis.-causing	5.17	1.71	8	VS (D)	Decreased (but not absent) P5CS protein in patient cultured fibroblasts (IF)
	<i>c.896C>T^o</i>	E8	p.(T299I)	G5K		Benign	0.148	0.692	Polymorph.	3.69	0.81		Trivial	
6/1 ¹²	<i>c.332A>G</i> (homozygous)	E4	p.(E111G) (homozygous)	G5K	ARCL3A	Prob.damaging	0.996	0.924	Dis.-causing	4.28	-0.51	8	VS	
7/7 ¹⁹	<i>c.359T>C</i> (monoallelic)	E4	p.(V120A) WT	G5K	SPG9A	Prob.damaging	0.995	0.858	Dis.-causing	4.28	-0.85	0-3	m (D)	↓Glu-to-Pro flow in cultured patient fibroblasts
8/1 sporadic ¹⁸	<i>c.377G>A</i> (monoallelic)	E4	p.(R126H) WT	G5K	ADCL3	Possib.damaging	0.614	0.663	Dis.-causing	5.17	0.12	7	S (D)	
9/1 ²⁵	<i>c.[30C>A;383G>A]</i> (homozygous)	E2	p.(F10L;R128H)	Mito. targeting; G5K	SPG9B	F10L: Benign	0.017	0.107	Polymorph.	0.97	-0.50	3	R128H: m	
		E4	(homozygous)			R128H:Prob.dam	0.978	0.693	Dis.-causing	5.17	0.37			
10/4 ¹⁹	<i>c.383G>A</i>	E4	p.(R128H)	G5K	SPG9B	Prob.damaging	0.978	0.693	Dis.-causing	5.17	0.37	7		
	<i>c.1910T>C</i>	E15	p.(L637P)	G5PR		Prob.damaging	1.000	0.968	Dis.-causing	4.81	-0.51		VS	
11-13 sporadic ¹⁶	<i>c.412C>T</i> (monoallelic)	E4	p.(R138W) WT	G5K	ADCL3	Prob.damaging	1.000	0.825	Dis.-causing	0.24	-0.67	7-9 1 dead 3y	S (D)	R138 not conserved in plants/bacteria, maps in a loop that is shorter in plants/bacteria. p.R138W: normal level (fibroblasts; IF, WB); subtly altered distribution in mitochondria (IF); hybrid WT-mutant tetramers formed, but ↓ mass in native electrophoresis; ↓Glu-to-Pro flow in patient fibroblasts ¹⁶
14,15 sporadic ¹⁶	<i>c.413G>T</i> (monoallelic)	E4	p.(R138L) WT	G5K	ADCL3	Prob.damaging	0.998	0.860	Dis.-causing	5.17	-0.67	7	S (D)	
16-19 spo ^{16,17}	<i>c.413G>A</i> (monoallelic)	E4	p.(R138Q) WT	G5K	ADCL3	Prob.damaging	0.997	0.737	Dis.-causing	5.17	-0.67	7	S (D)	
20/1 ²⁷	<i>c.725G > A</i> (homozygous)	E7	p.(S242N) (homozygous)	G5K	SPG9B	Possib.damaging	0.493	0.720	Dis.-causing	5.30	0.20	2	Vm	Normal levels and mitochondrial localization of P5CS ^{S242N} protein in transfected Hela (IF) and HEK293 cells (WB).
21/12 ^{20,22}	<i>c.727G>C</i> (monoallelic)	E7	p.(V243L) WT	G5K	SPG9A	Benign	0.001	0.665	Dis.-causing	1.46	-0.29	1-3	m-Vm (D)	Modest ↓ in P5CS protein level (WB) with normal cell localization (IF). ↓↓↓ activity (RP). Disturbs P5CS architecture ²⁰
22/9 ^{20,21} 23/1 spo ¹⁹ 24/4 ¹⁹	<i>c.755G>A</i> (monoallelic)	E7	p.(R252Q) WT	G5K	SPG9A	Prob.damaging	0.941	0.734	Dis.-causing	5.35	0.09	1-4	M-Vm (D)	Proper production and cell localization of mutant P5CS. ↓↓↓ activity (RP). Disturbs P5CS architecture ²⁰
25/2 ²⁶	<i>c.1112G>A</i>	E10	p.(R371Q)	G5PR	SPG9B	Prob.damaging	1.000	0.623	Dis.-causing	5.04	-0.25	5	??	For both mutations 80% decrease in the V _{max} for the G5PR partial activity of P5CS (RP)
	<i>c.1490G>A</i>	E10	p.(S497N)	G5PR		Prob.damaging	0.998	0.791	Dis.-causing	2.75	-0.82		??	
26/1 ¹⁴	<i>c.1273C>T</i>	E12	p.(R425C)	G5PR	ARCL3A	Prob.damaging	1.000	0.849	Dis.-causing	5.15	-1.26	9?	VS	
	<i>c.177delG</i>	E3	p.(K59Nfs*9)	100%G5K+G5PR		NA	NA	NA	Dis.-causing	NA	NA	Foetus		

27/2 ⁶ 28/1 ⁷	<i>c.1273C>T</i> <i>c.2225G>T</i>	E12 E18	p.(R425C) p.(S742I)	G5PR G5PR	ARCL3A	Prob.damaging Prob.damaging	1.000 1.000	0.849 0.961	Dis.-causing Dis.-causing	5.15 5.05	-1.26 -1.18	7 I	
29/1 ¹⁰	g.97373623-97372101del (homozygous)	I14-E15-I15	p.(V601Gfs*24) (homozygous)	50% G5PR	ARCL3A	NA	NA	NA	Dis.-causing	NA	NA	10	90% decrease of normal mRNA for P5CS and lack of P5CS protein in cultured fibroblasts from patient (WB)
30/1 ²³	<i>c.1864C>T</i> <i>c.1988C>A</i>	E15 E16	p.(R622W) p.(S663*)	G5PR 30% G5PR	SPG9B	Prob.damaging NA	0.967 NA	0.72 NA	Dis.-causing Dis.-causing	1.31 5.17	1.19 NA	9 Dead 4y	VS ↓fibroblasts growth if Pro not added. P5CS protein in fibroblasts: 2% of normal (PROT)
31/1 ⁵	<i>c.1923+1G>A</i> (homozygous)	I15	p.(M586I del587_657) and p.(V601Gfs*24) ^p	16% G5PR lost ^d 50% G5PR lost ^d	ARCL3A	NA	NA	NA	Dis.-causing	NA	NA	10 Dead 6m	Lack of normal mRNA and P5CS protein in cultured fibroblasts (IF, WB). Loss of catalytic Cys612 in both forms
32/1 sporadic ¹⁹	<i>c.1955C>T</i> (monoallelic)	E16	p.(S652F) WT	G5PR	SPG9A	Possib.damaging	0.694	0.818	Dis.-causing	5.17	1.52	2	Vm (D)
33/2 ²⁵	<i>c.1994G>A</i> <i>c.1321C>T</i>	E16 E12	p.(R665Q) p.(R441*)	G5PR 80% G5PR	SPG9B	Possib.damaging NA	0.78 NA	0.560 NA	Dis.-causing Dis.-causing	5.17 3.63	1.69 NA	6??	M??
34/2 ¹⁹	<i>c.1994G>T</i> (monoallelic)	E16	p.(R665L) WT	G5PR	SPG9A	Possib.damaging	0.78	0.824	Dis.-causing	5.17	1.69	3	m (D)
35/1 ¹⁰	<i>c.2131delC</i> (homozygous)	E17	p.(L711Cfs*3) (homozygous)	20% G5PR	ARCL3A	NA	NA	NA	Dis.-causing	NA	NA	10 Dead 3m	
36/2 ¹⁹	<i>c.2143G>C</i> (homozygous)	E17	p.(D715H) (homozygous)	G5PR	SPG9B	Prob.damaging	0.999	0.948	Dis.-causing	5.59	-1.05	5	M
37/2 ¹³	<i>c.2177G>A</i> <i>c.298G>T</i>	E17 E3	p.(R726H) p.(E100*)	G5PR 90% G5K+G5PR	ARCL3A	Prob.damaging NA	1.000 NA	0.937 NA	Dis.-causing Dis.-causing	5.59 5.17	-1.04 NA	9 Dead 2y	VS
38/2 ⁹	<i>c.2246G>A</i> <i>c.2294G>A</i>	E18 E18	p.(R749Q) p.(R765Q)	G5PR G5PR	ARCL3A	Prob.damaging Benign	0.999 0.163	0.823 0.634	Dis.-causing Dis.-causing	5.05 5.00	-1.19 1.47	7-8	Probably S Probably S Normal mRNA levels but decreased (but not absent) P5CS protein level (WB) in patient cultured fibroblasts. Inferred ↓ P5CS stability
39/1 ⁸	<i>c.2345A>G</i> (homozygous)	E18	p.(Y782C) (homozygous)	G5PR	ARCL3A	Possib.damaging	0.859	0.896	Dis.-causing	4.15	-0.17	7.5	S
40/4 ⁴	<i>c.2350C>T</i> (homozygous)	E18	p.(H784Y) (homozygous)	G5PR	ARCL3A	Prob.damaging	0.933	0.863	Dis.-causing	5.00	-1.16	7	S Report of apparently normal level and cell localization of P5CS (IF) and normal Glu→Pro flow in patient cultured fibroblasts

Families have been numbered from lower to higher values corresponding to the position of the mutation believed to be disease-causing along the gene sequence. In compound heterozygotes the order is given by the most upstream (expectedly) disease-causing allele. To facilitate distinction between the different syndromes, rows for patients and families presenting ARCL3A, ADCL3, SPG9B and SPG9B are colored darker and lighter red and darker and lighter blue, respectively. NA, not applicable.

^aThe superscript figures give the references (listed in the main text) where patients and families were reported. Spo or sporadic, sporadic patient.

^b GeneBank (<https://www.ncbi.nlm.nih.gov/nucleotide/>) reference sequences for human *ALDH18A1* gene, its mRNA (isoform 1, long form) and protein (long form), NG_012258.1, NM_002860.3 and NP_002851.2, respectively. Nucleotide numbering uses +1 as the A of the ATG translation initiation codon (codon1). When the mutation affects a CpG dinucleotide, the nucleotide change is shown in italic type.

^cE/I, exon/Intron

^dUniprot (KB <https://www.uniprot.org/uniprot/>) reference number P54886. WT, wild type.

^eMitoch, mitochondrial targeting sequence, residues 1-57. G5K, glutamate 5-kinase component, residues 58-354; G5PR, glutamate 5-phosphate reductase component, residues 362-795. For mutations causing P5CS truncations, the percentage of domain loss is indicated.

^fARCL3A, recessive cutis laxa type IIIA (MIM #219150); ADCL3, dominant cutis laxa type 3 (MIM # 616603); SPG9A, dominant spastic paraplegia or paraparesis due to mutations in *ALDH18A1* (MIM#601162); SPG9B, recessive spastic paraplegia or paraparesis due to mutations in *ALDH18A1* (MIM#616586).

^g Polyphen-2 (HumVar-trained dataset; <http://genetics.bwh.harvard.edu/pph2>) grades the probability of a damaging effect of an amino acid change, as Probably damaging (*Prob.damag.* or *damaging*), Possibly damaging (*Possib.damaging*) and *benign*. Highest probability score is 1.

^h The score given by MutPred2 (<http://mutpred.mutdb.org/>) is the probability that a given amino acid change is deleterious/disease associated.

ⁱ Mutation Taster (<http://www.mutationtaster.org/>) predicts if an alteration is Probably deleterious (Dis.-causing) or Probably harmless (polymorphis, abbreviated polymorph.).

^j PhyloP (calculated by Mutation taster) measures evolutionary conservation at individual alignment sites providing positive scores (maximum 6) at sites that are predicted to be conserved or negative scores (mínimum -14) when sites are predicted to evolve fast.

^k Amino acid conservation estimate by the ConSurf server (<https://consurf.tau.ac.il/>). The more negative the value, the higher the conservation of a residue. 0, rate of evolution corresponding to the average for the entire sequence. Postive values, increased rate of evolution (low conservation).

^l Clinical severity in a scale from low to high (0 to 10) according to the reported information on the affected patients. When the reported information is scarce for a sound judgement, the proposed figure is shown with question marks.

^m The severity of a given missense mutation is inferred from the clinical severity in patients with informative genotypes (for example homozygosity for the mutation, compound heterozygosity with a null allele or with a mutant allele of known severity inferred from another genotype). VS, S, I, M, m and Vm: very severe, severe, intermediate, modest, mild and very mild, respectively, in decreasing order of severity, in which very severe is approximately identical to a null mutation and very mild may give no manifestations in some patients of a family or the manifestations may be observed only in special circumstances such as pregnancy. When no inference can be made for a given mutation, question marks are shown. The term trivial is applied to a polymorphism without known phenotypic repercussion. (D) stands for dominant character.

ⁿ Abbreviations: IF, immunofluorescence; WB, western blot; RP, assays in recombinant P5CS produced *in vitro*.

^o Considered a polymorphism. Allele frequency > 10% annotated at the GNOMAD database (https://gnomad.broadinstitute.org/gene/ENSG00000059573?dataset=gnomad_r2_1).

^p Two alternative forms produced from the same splicing error.

^q Catalytic Cys612 lost in both forms